8-15-1961

A Study of a Nonlinear Compensation Network in a Feedback Control System

John F. Taylor

A STUDY OF A NONLINEAR COMPENSATION NETWORK IN A FEEDBACK CONTROL SYSTEM - TAYLOR

A STUDY OF A NONLINEAR COMPENSATION NETWORK IN A FEEDBACK CONTROL SYSTEM

By

John F. Taylor

A Thesis

Submitted in Partial Fulfillment of the

Requirements for the Degree of

Master of Science in Electrical Engineering

The University of New Mexico

1961

This thesis, directed and approved by the candidate's committee, has been accepted by the Graduate Committee of the University of New Mexico in partial fulfillment of the requirements for the degree of

MASTER OF SCIENCE

E. A. Castetter

Dean

August 15, 1961

Date

A STUDY OF A NONLINEAR COMPENSATION NETWORK IN A FEEDBACK CONTROL SYSTEM

By

John F. Taylor

Thesis committee

Arnold H. Kochmann

Chairman

W. W. Koepsel

Ruben D. Kelly

TABLE OF CONTENTS

ACKNOWLEDGEMENTS

The author wishes to express his appreciation to his thesis advisor, Dr. Arnold H. Koschmann, for his many helpful suggestions and his patient guidance during the past year.

John F. Taylor

LIST OF TABLES

LIST OF FIGURES

FIGURE PAGE

FIGURE PAGE

CHAPTER I

INTRODUCTION

This paper is a study of the effect of a nonlinear compensation network on the closed-loop response of a feedback control system.

Physical energy dissipation elements, unlike their usual mathematical models, are often nonlinear. An example of such a nonlinear element is the mechanical damper. Since dissipation elements are used in most types of compensation, the problem of nonlinear compensation is an important one.

The study was performed with two goals in mind. The first was to determine the detrimental effects resulting from the insertion of the nonlinear network. The second was to see if any improvement in system performance could be realized by the insertion.

In order to keep the problem within reasonable limits and to obtain definite results, a specific example was considered. An electrical system was used, but the results of the study can be extended to other types of systems by means of the various sets of physical analogies.

The nonlinear element used in the study was a resistance which obeys the nonlinear relation

$$v = k\, i|i| \tag{1.1}$$

instead of Ohm's law. The symbol for this element is shown in Figure 1.

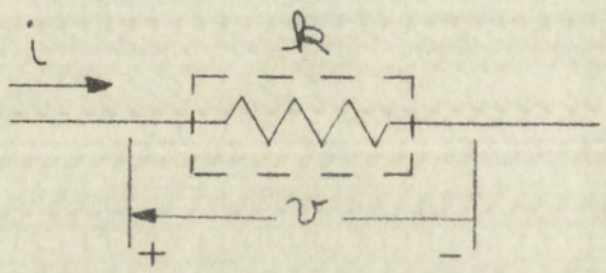

Figure 1.--Symbol for nonlinear resistance element

The control system which was used is shown in Figure 2. This system is discussed in Truxal's Automatic Feedback Control System Synthesis.[1] Truxal sets certain specifications on the closed-loop system and then attempts to design a compensation network which will yield these specifications. The desired specifications are:

$$K_v \leqslant 10/\text{second} \tag{1.2}$$

$$\text{Overshoot of step-function response} \leqslant 30\% \tag{1.3}$$

Suitable compensation is provided by the RC network shown in Figure 3, where

$$C = 10 \text{ microfarads}$$
$$R_1 = 18.666 \text{ megohms} \qquad R_2 = 1.333 \text{ megohms} \tag{1.4}$$

---

[1] John G. Truxal, Automatic Feedback Control System Synthesis (New York: McGraw-Hill Book Company, Inc., 1955), pp. 251-254.

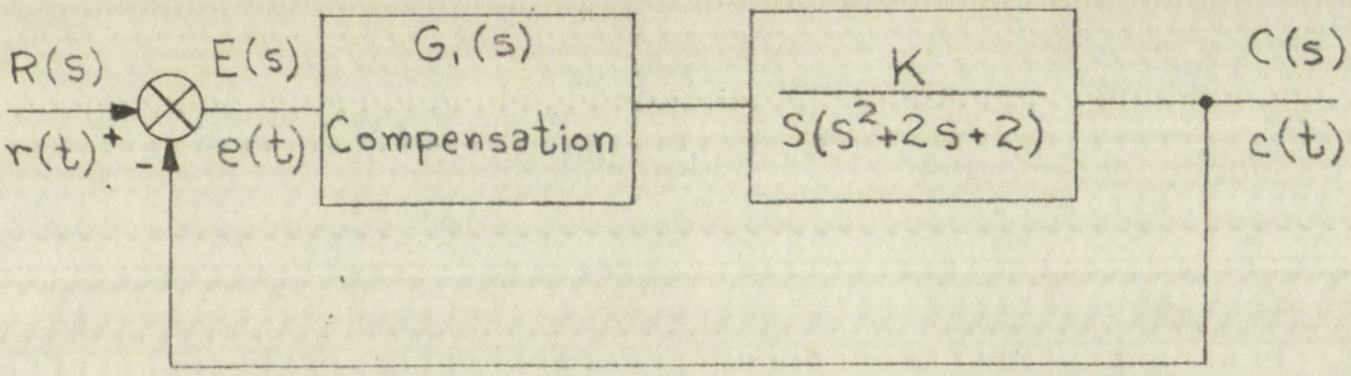

Figure 2.--Control system used in study

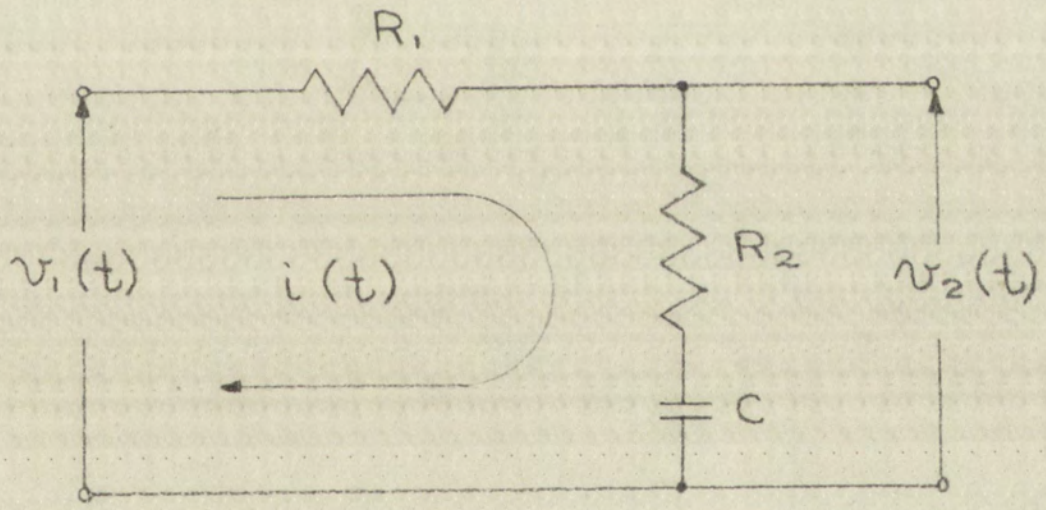

Figure 3.--RC compensation network

This network has the transfer function

$$G_1(S) = \frac{1}{15}\,\frac{S+.075}{S+.005} \qquad (1.5)$$

When this network is used, setting the gain at K = 20 yields a system which meets the desired specifications.

When the nonlinear resistance element described by equation (1.1) is inserted in the network shown in Figure 3, three nonlinear networks are possible. They are shown in Figure 4.

The values of the parameters which were used are:

$$\begin{aligned} R_1 &= 18.666 \text{ megohms} \\ R_2 &= 1.333 \text{ megohms} \\ C &= 10 \text{ microfarads} \\ k_1 &= 18.666 \times 10^{12} \text{ ohms/ampere} \\ &= 18.666 \text{ megohms/microampere} \\ k_2 &= 1.333 \times 10^{12} \text{ ohms/ampere} \\ &= 1.333 \text{ megohms/microampere} \end{aligned} \qquad (1.6)$$

The values of k_1 and k_2 were chosen so that when the current, i, is one microampere, the d-c resistance of each nonlinear element is the same as that of the corresponding linear element.

It is shown in Appendix A that the results of the study may be extended to include networks with other values of k_1 and k_2.

The three closed-loop systems resulting from the use of Networks A, B, and C as compensation for the system shown in Figure 2 were each studied separately. Two aspects of system

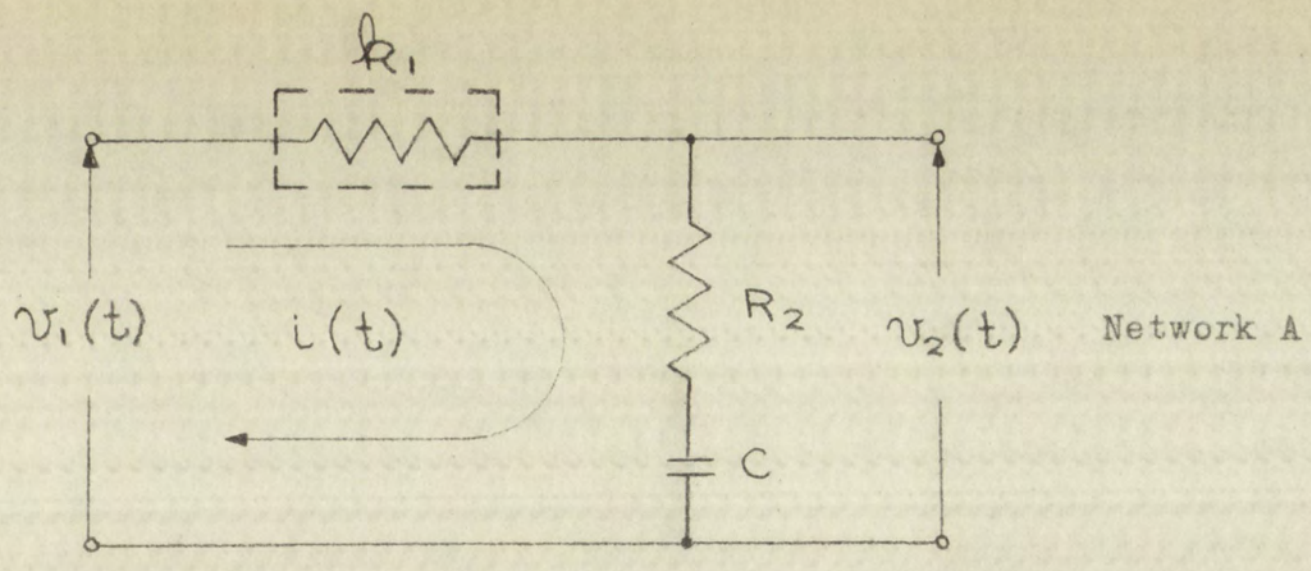

Network A

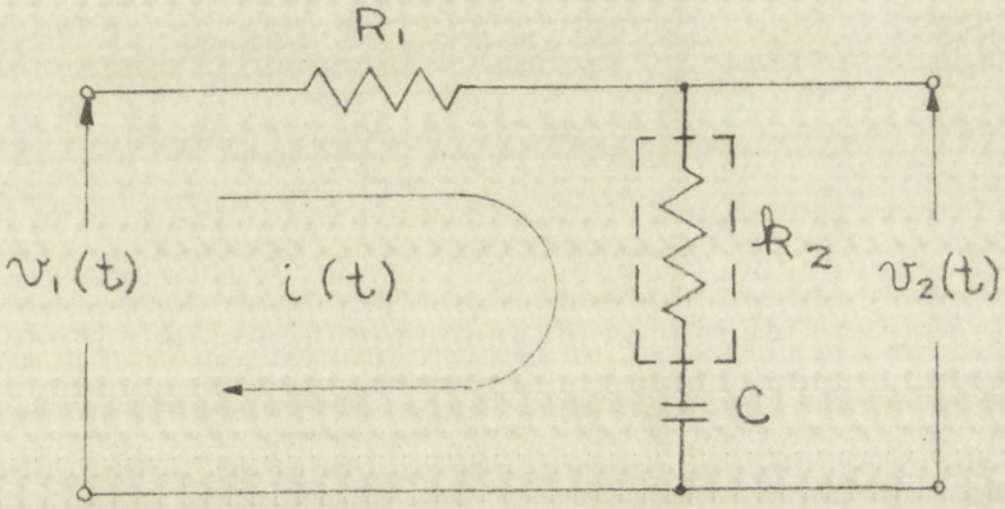

Network B

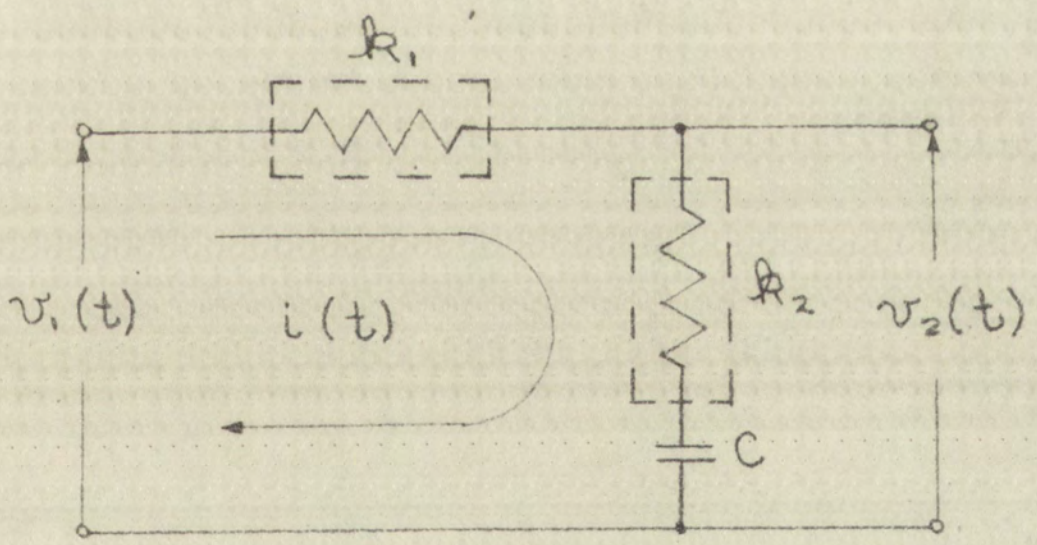

Network C

Figure 4.--RC network of Figure 3 with nonlinear resistance elements inserted

performance were considered, the stability of the closed-loop and the step-function response. The step responses of the nonlinear systems were compared with the response of the linear system resulting from the use of the network shown in Figure 3, page 3, as compensation.

The stability of each system was investigated by both analytic means and by analog computer simulation. The step-function responses were studied by means of computer simulation.

CHAPTER II

STABILITY ANALYSIS

Stability is a rather well-defined concept in the linear system. A linear system is either stable or unstable, and the stability depends only on the system parameters; it is independent of the input.

In the case of nonlinear systems, however, the question of stability is much more complex. It depends not only on the system parameters, but also on the excitation. Another phenomenon which occurs in the nonlinear system but not in the linear one is the limit cycle, or sustained oscillation. The limit cycle may or may not be sinusoidal. These concepts will be discussed further below.

I. THE DESCRIBING FUNCTION APPROACH

One way of investigating the stability of a nonlinear system is the describing function approach. This method is an attempt to extend the concept of the transfer function to the nonlinear system. It was first used in connection with contactor servomechanisms.[1]

The describing function of a nonlinear device is defined as follows. If the input to the device is given by

$$V \sin \omega t \tag{2.1}$$

---

[1] R. J. Kochenburger, "A Frequency Response Method for Analyzing and Synthesizing Contactor Servomechanisms," Transactions of the A.I.E.E.-Part I, LXIX (1950), 270-284.

then the output, if the system is stable, is of the form

$$C_o + \sum_{m=1}^{\infty} C_m \sin(\omega t + \theta_m) \qquad (2.2)$$

The describing function of the device, $N(V,\omega)$ is defined as[2]

$$N(V,\omega) = \frac{C_1}{V} \angle \theta_1 \qquad (2.3)$$

In some cases, N is a function only of V, but in the most general case it also depends on frequency.

The describing function may be used in finding whether a limit cycle can exist provided certain conditions are met. Consider the system shown in Figure 2, page 3, where the compensation is a nonlinear device with a describing function $N(V,\omega)$. For the ordinary nonlinear device, the fundamental component in equation (2.2) is larger than the harmonics. Furthermore, the harmonics are attenuated more than the fundamental because of the low-pass characteristics of the linear portion of the system. Thus, the fundamental component of the output of the nonlinear portion contributes much more to c(t) and e(t) than do the harmonics. Under these conditions the loop gain is approximately[3]

$$N(V,\omega)\, G(j\omega) \qquad (2.4)$$

---

[2]Gordon J. Murphy, Control Engineering (New York: D. Van Nostrand Company, Inc., 1959), pp. 310-311.

[3]John G. Truxal, Automatic Feedback Control System Synthesis (New York: McGraw-Hill Book Company, Inc., 1955), p. 574.

where

$$G(j\omega) = \frac{K}{S(S^2+2S+2)}\Big|_{S=j\omega} \qquad (2.5)$$

Hence, a sustained oscillation may occur if[4]

$$-N(V,\omega) = \frac{1}{G(j\omega)} \qquad (2.6)$$

Graphical means may be used to determine whether such a condition can be met in a particular system. If it is met, the amplitude and frequency of the fundamental component of the oscillation can be predicted.

This can be most clearly seen by the use of an illustration. Consider a situation such as that shown in Figure 5, where $-N(V,\omega)$ and $1/G(j\omega)$ are plotted on the same set of axes. It is seen that the condition in equation (2.6) is met at two points, P_1 and P_2. Thus, sustained oscillations can exist at frequencies ω_2 and ω_5 with respective amplitudes V_2 and V_6.

Whether these oscillations are stable or not is another question. A rather convenient criterion is given in the literature.[5] Denoting the tangent to the $1/G(j\omega)$ curve in the direction of increasing ω by $\underline{\mathfrak{A}}$ and the tangent to the $-N(V,\omega)$ curve in the direction of increasing V by $\underline{\mathfrak{B}}$, the cross product $\underline{\mathfrak{A}} \times \underline{\mathfrak{B}}$ is formed. If $\underline{\mathfrak{A}} \times \underline{\mathfrak{B}}$ is positive, the sustained oscillation is

---

[4] Ibid., p. 575.

[5] J-C Gille, M. J. Pelegrin, and P. Decaulne, Feedback Control Systems (New York: McGraw-Hill Book Company, Inc., 1959), pp. 419-421.

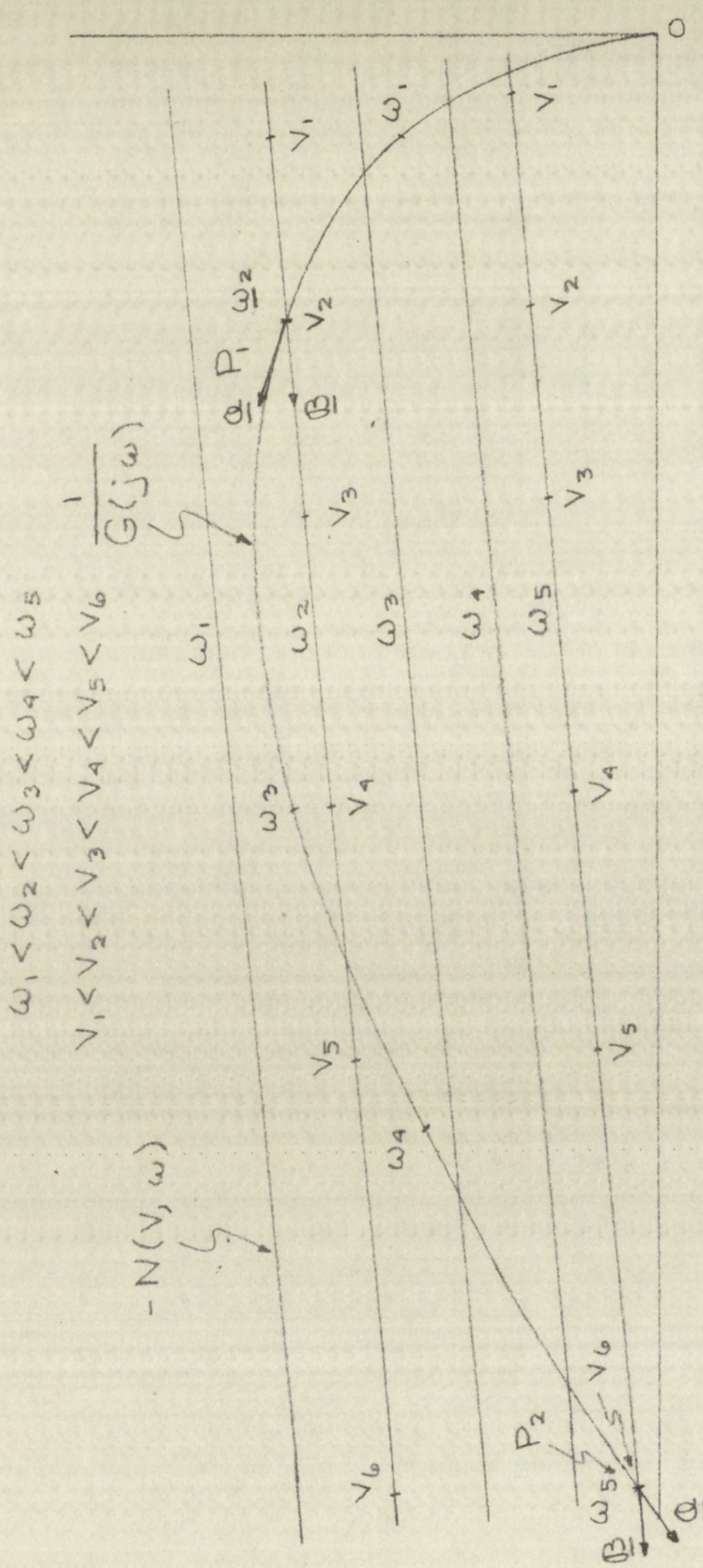

Figure 5.--Graphical determination of limit cycles

stable and is called a limit cycle. If $\underline{\mathbb{Q}} \times \underline{\mathbb{B}}$ is negative, the oscillation is unstable. For a stable equilibrium point, a decrease or increase in the amplitude of the oscillation alters the system characteristics in such a way that equilibrium is restored. With an unstable equilibrium point a decrease or increase in the amplitude of the oscillation causes the output to increase without bound or to settle into a stable oscillation at some other amplitude and frequency.

In Figure 5, P_1 is a stable equilibrium point and P_2 is an unstable equilibrium point.

It should be mentioned that at the points shown, an oscillation can be sustained, but there is no guarantee that any given input will excite such an oscillation. There is no existing theory to investigate this question.[6]

II. CALCULATION OF THE LIMIT CYCLES

The computation of the describing functions and the numerical results of these calculations are contained in Appendix B. The results are presented in this section in graphical form.

Figures 6 to 8 show the describing function for network A; Figures 9 to 11, for network B; and Figures 12 to 14, for network C. These figures are on pages 12 to 20.

---

[6] Eli Mishkin and Ludwig Braun, Jr. (ed.), Adaptive Control Systems (New York: McGraw-Hill Book Company, Inc., 1961), pp. 196-197.

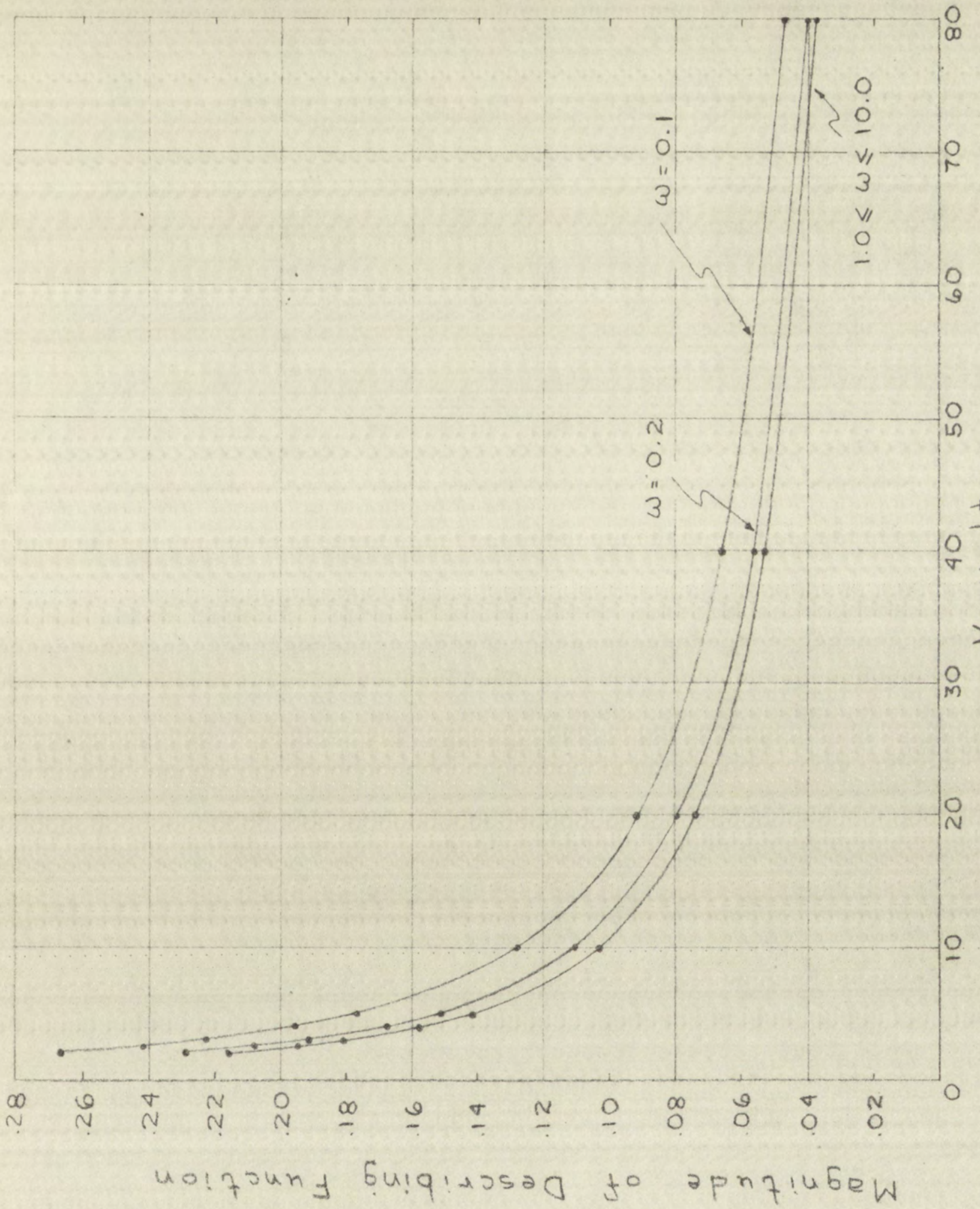

Figure 6.--Magnitude of describing function for network A versus V.

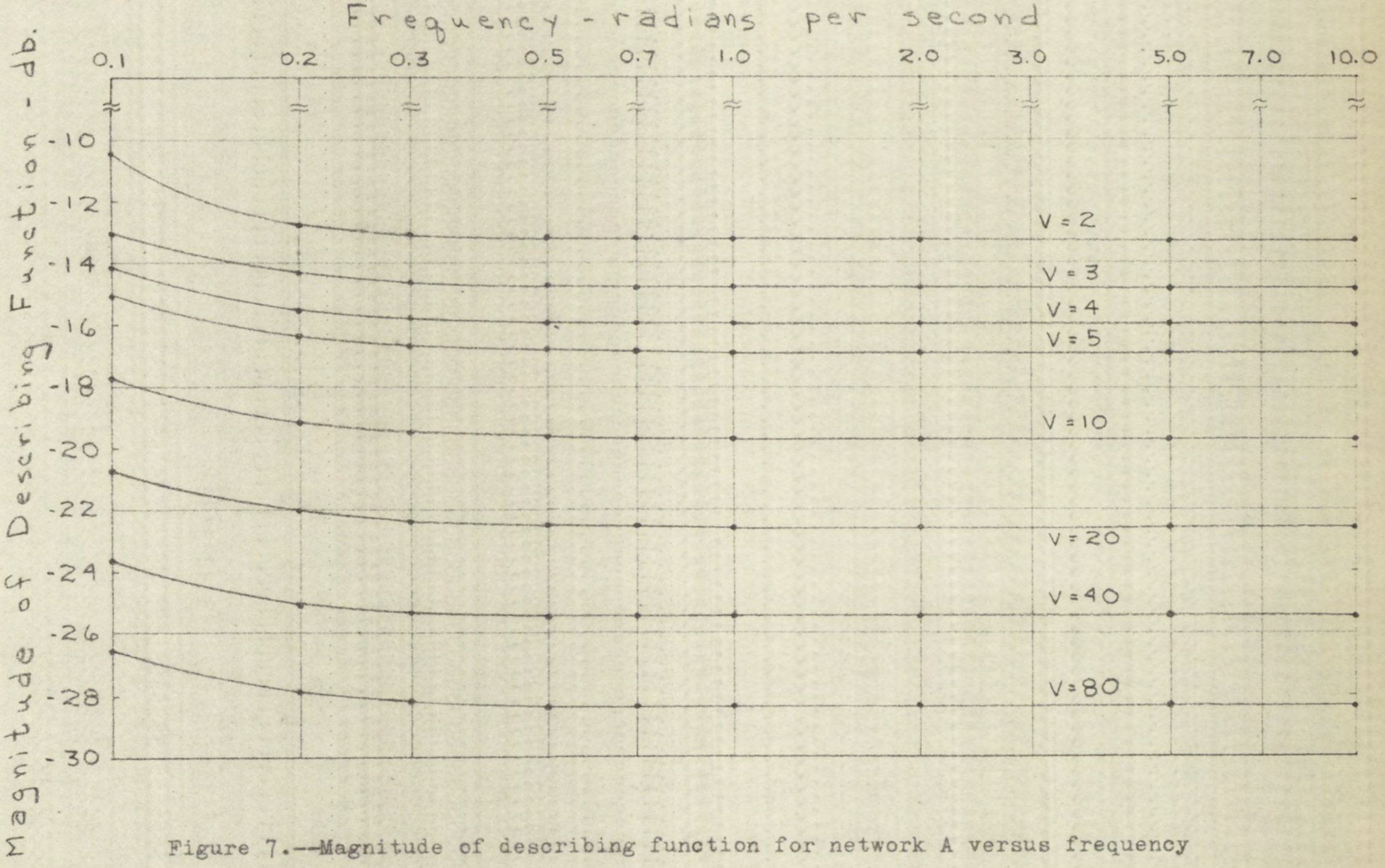

Figure 7.--Magnitude of describing function for network A versus frequency

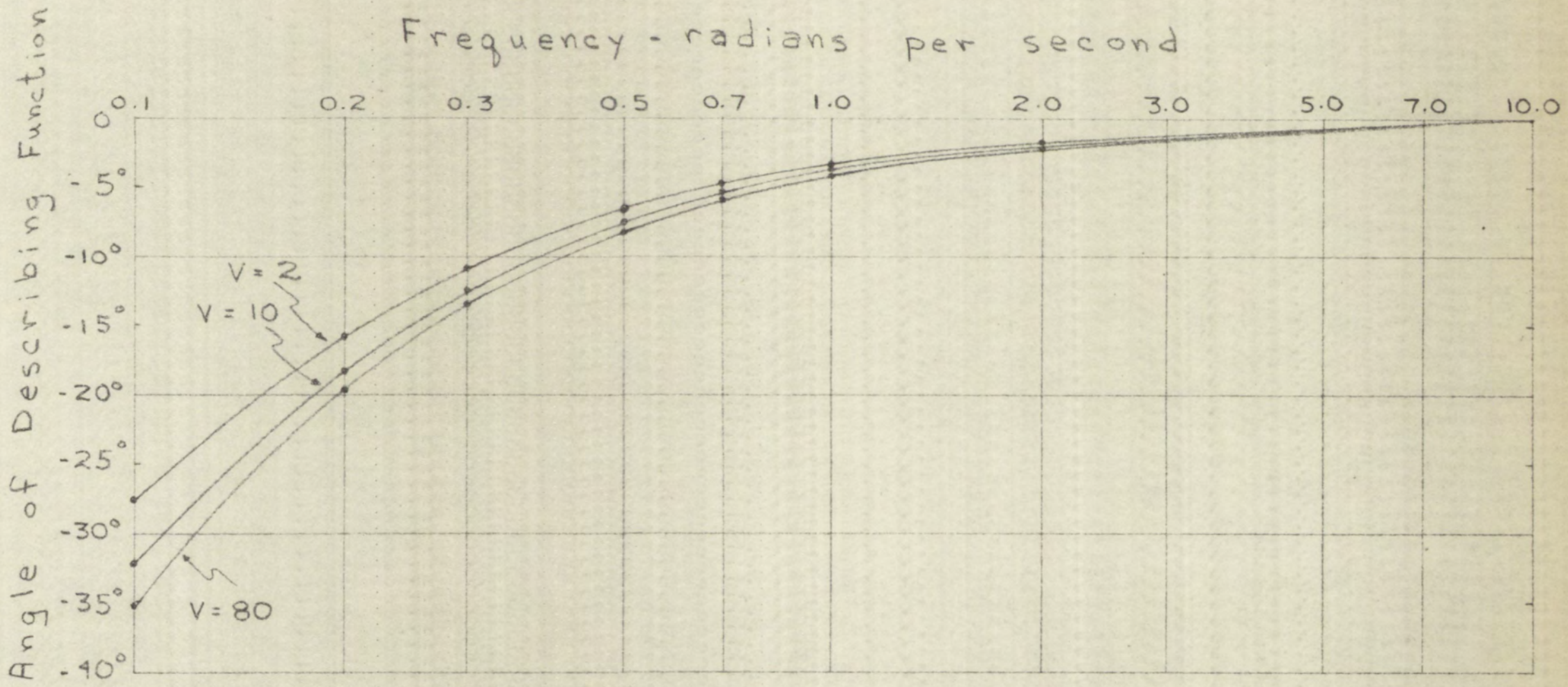

Figure 8.--Angle of describing function for network A versus frequency

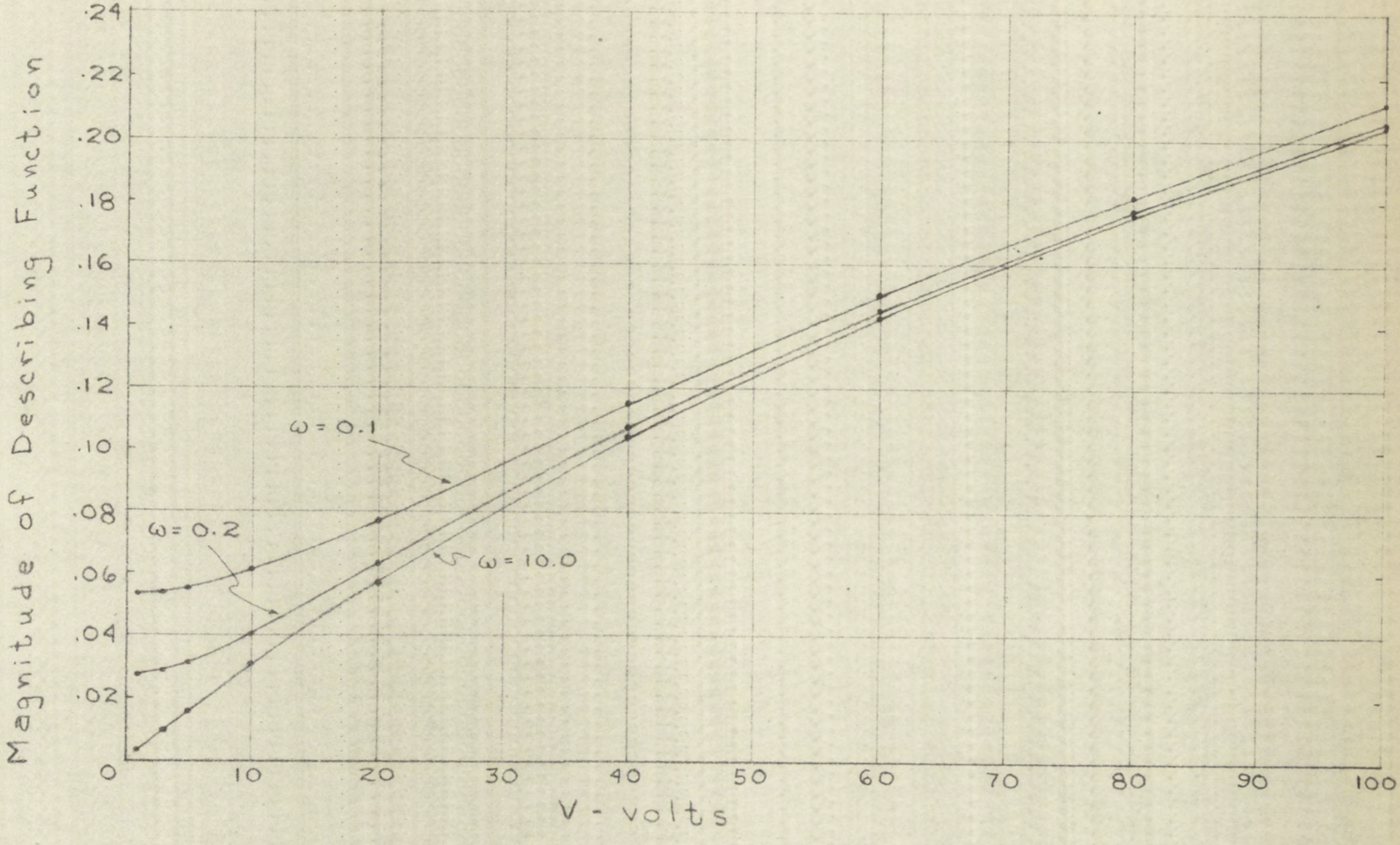

Figure 9.--Magnitude of describing function for network B versus V

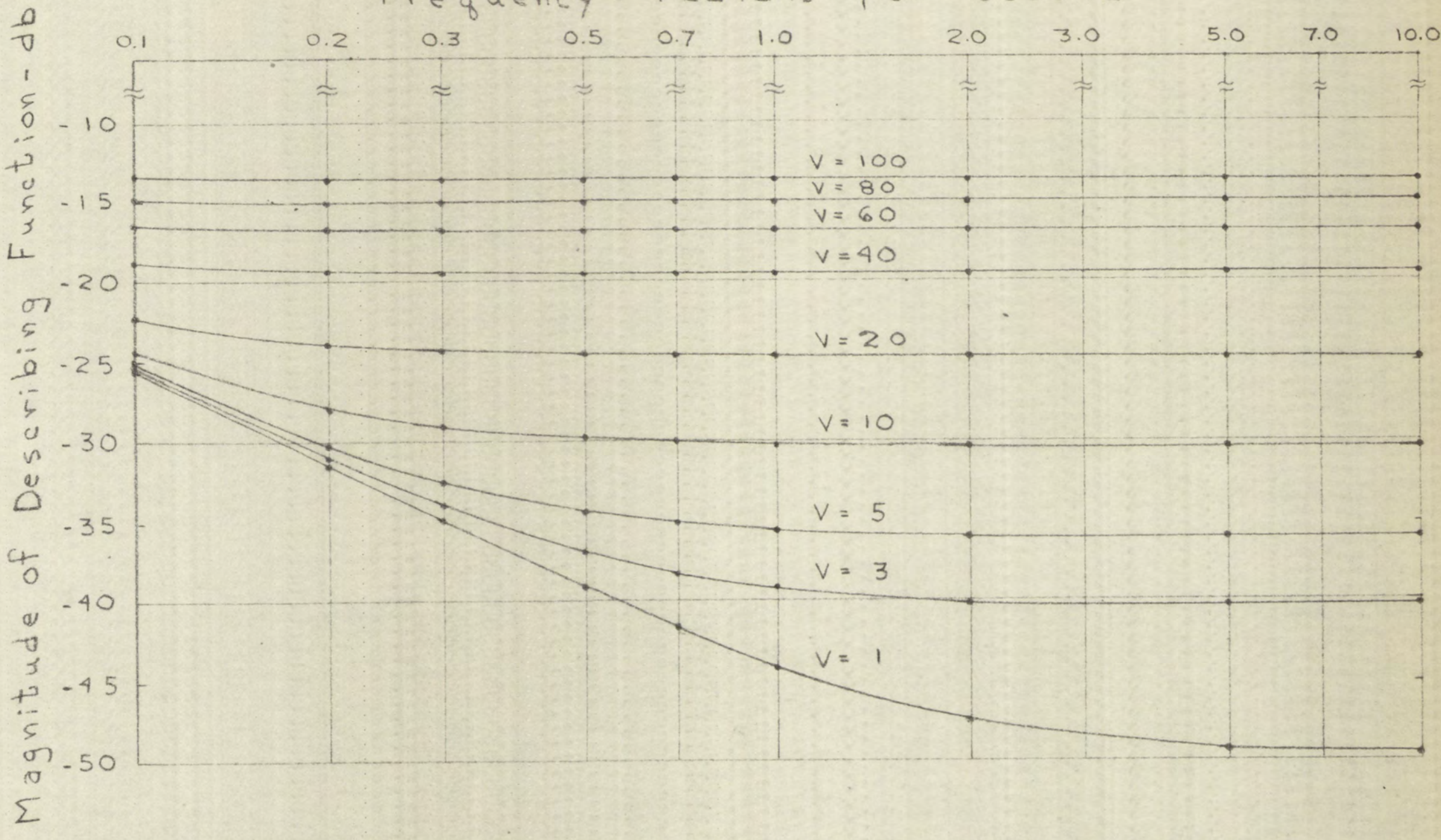

Figure 10.--Magnitude of describing function for network B versus frequency

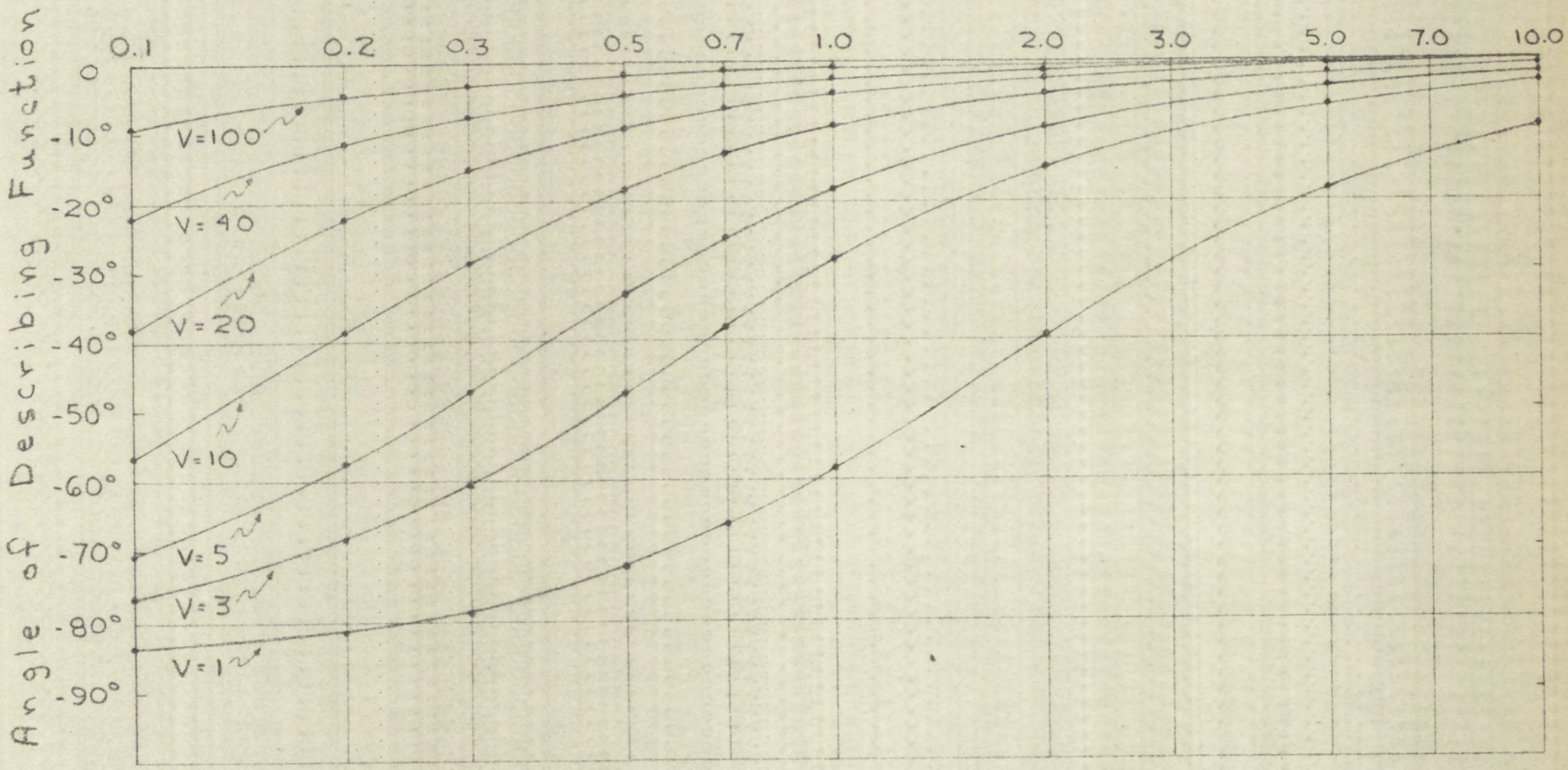

Figure 11.--Angle of describing function for network B versus frequency

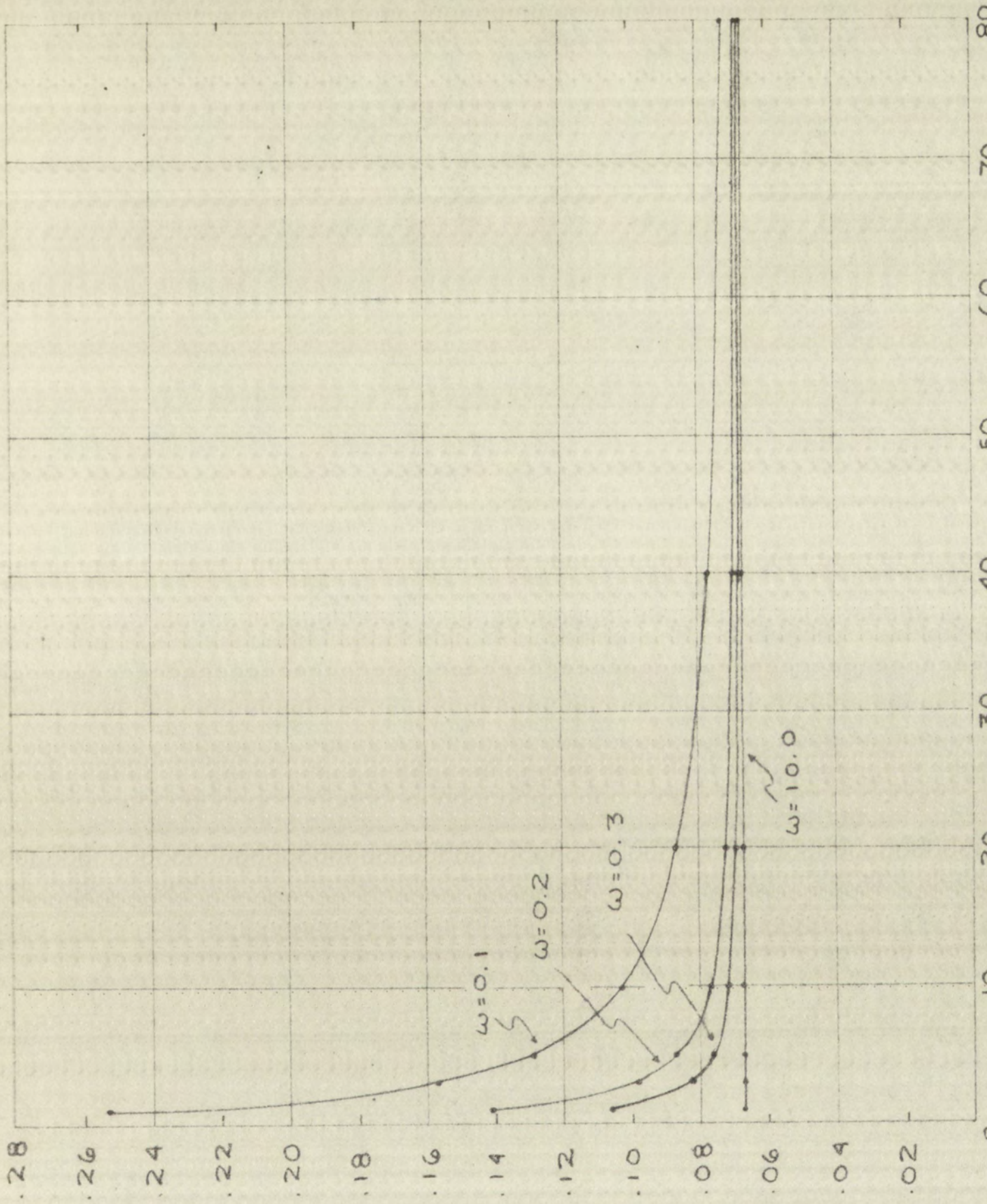

Figure 12.--Magnitude of describing function for network C versus V

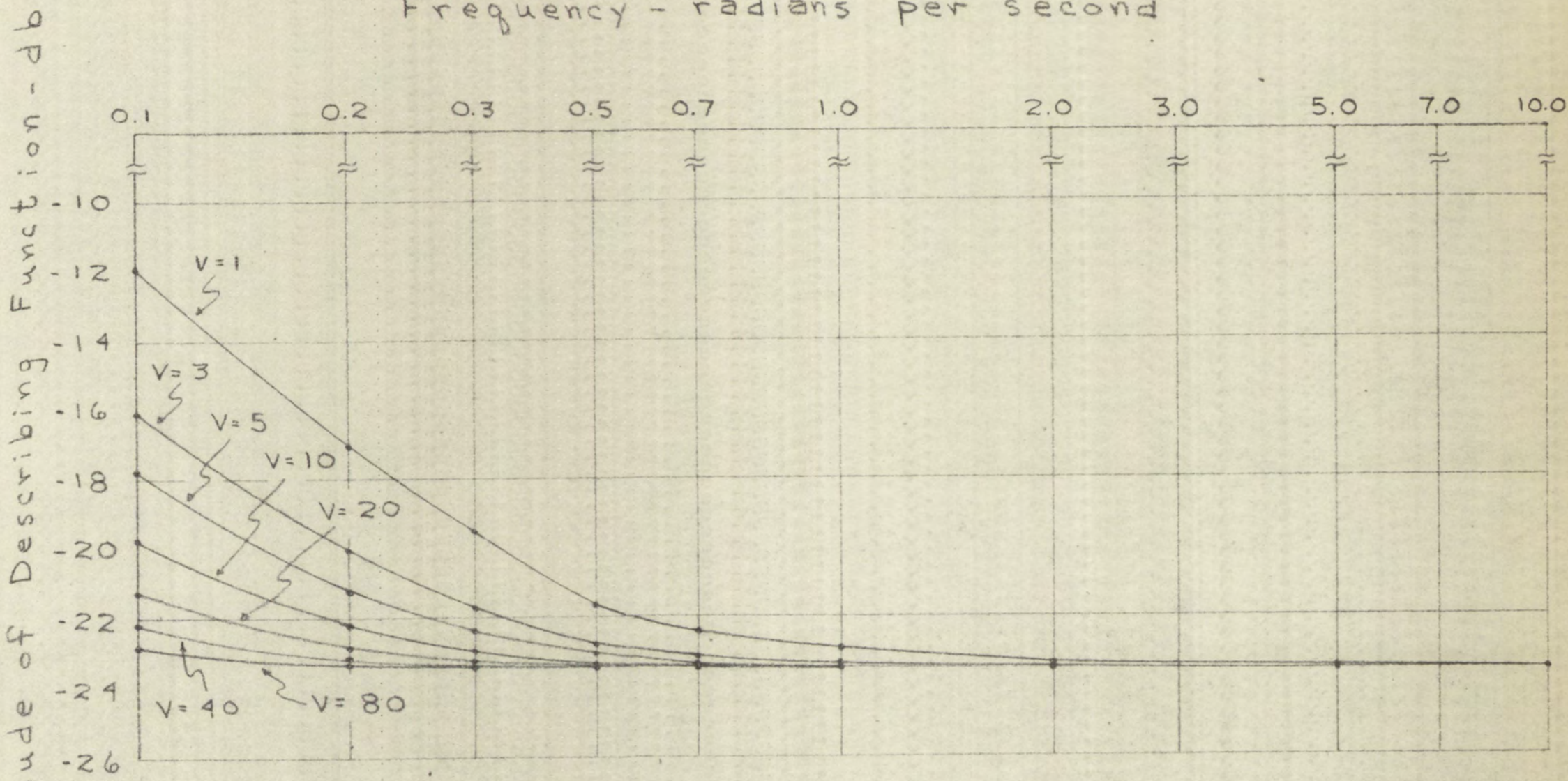

Figure 13.--Magnitude of describing function for network C versus frequency

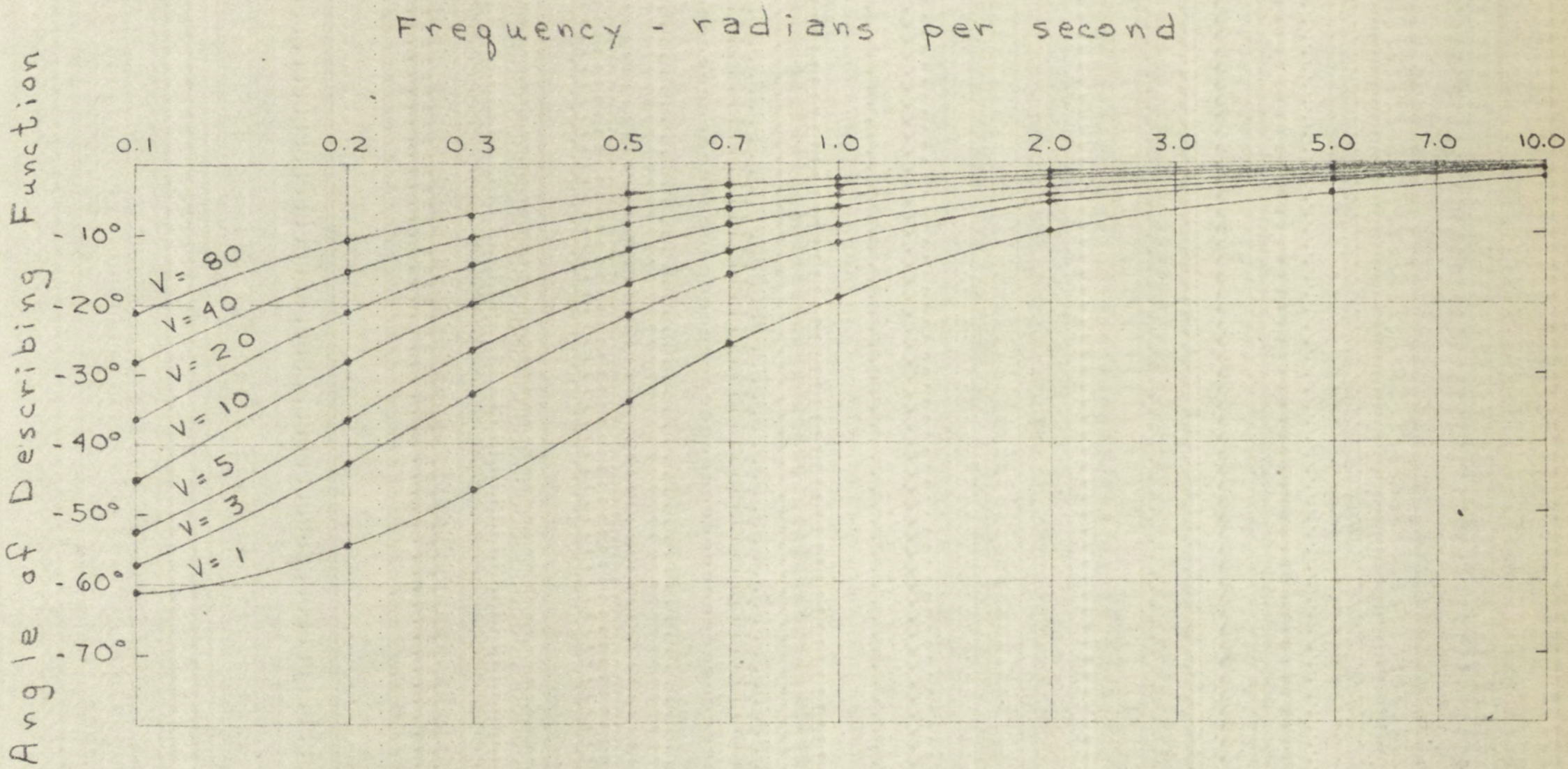

Figure 14.--Angle of describing function for network C versus frequency

System A

Using these results, the limit cycles may be calculated. Figure 15 is a polar plot of $1/G(j\omega)$ superimposed on a plot of $-N(V,\omega)$ for network A. This plot is used to find the limit cycles for the nonlinear closed-loop system resulting from the employment of network A as compensation for the system shown in Figure 2, page 3. It is seen from Figure 15 that there is only one point where the condition $-N(V,\omega) = 1/G(j\omega)$ is met. This is in the neighborhood of $\omega = 1.4$ on the $1/G(j\omega)$ locus. The actual intersection occurs at $\omega = 1.37$ radians per second. The manner in which the curves cross each other indicates that the equilibrium point is a stable one. Figure 16, page 23, shows the polar plot of the describing function for $\omega = 1.37$ superimposed on plots of $1/G(j\omega)$ for various values of K. It is seen here that for all values of K, the frequency at the equilibrium point is 1.37 radians per second. The approximate amplitude of the oscillation may be read directly from the describing function curve. More accurate values may be found by finding the magnitude of the describing function at the equilibrium point and then finding the voltage corresponding to this magnitude from the curves in Figure 6, page 12.

Table 1, page 24, gives the amplitudes and frequencies of the limit cycles for several values of K. These values are compared with those obtained by computer simulation in Section III of this chapter.

System B

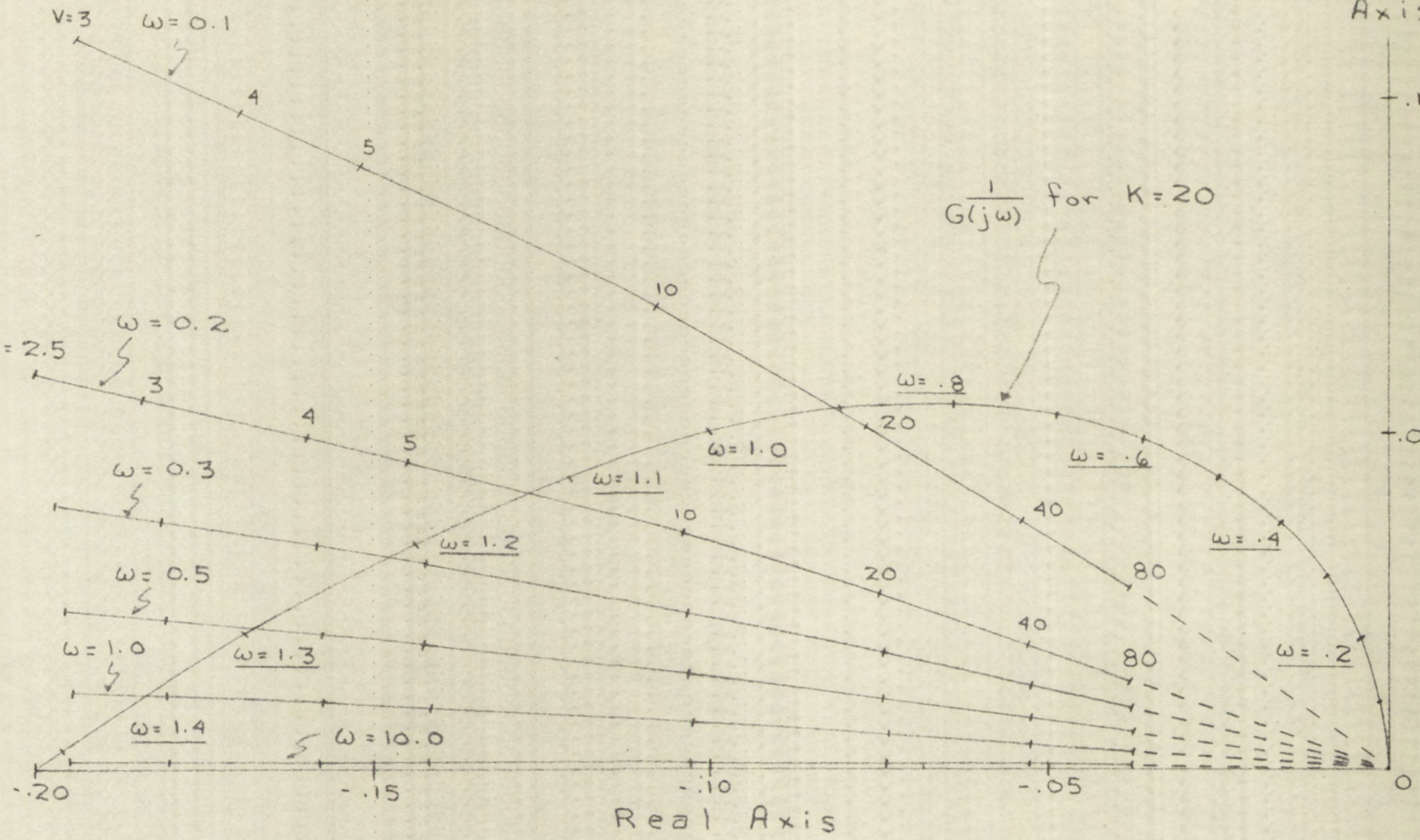

Figure 15.--Polar plot of describing function for network A

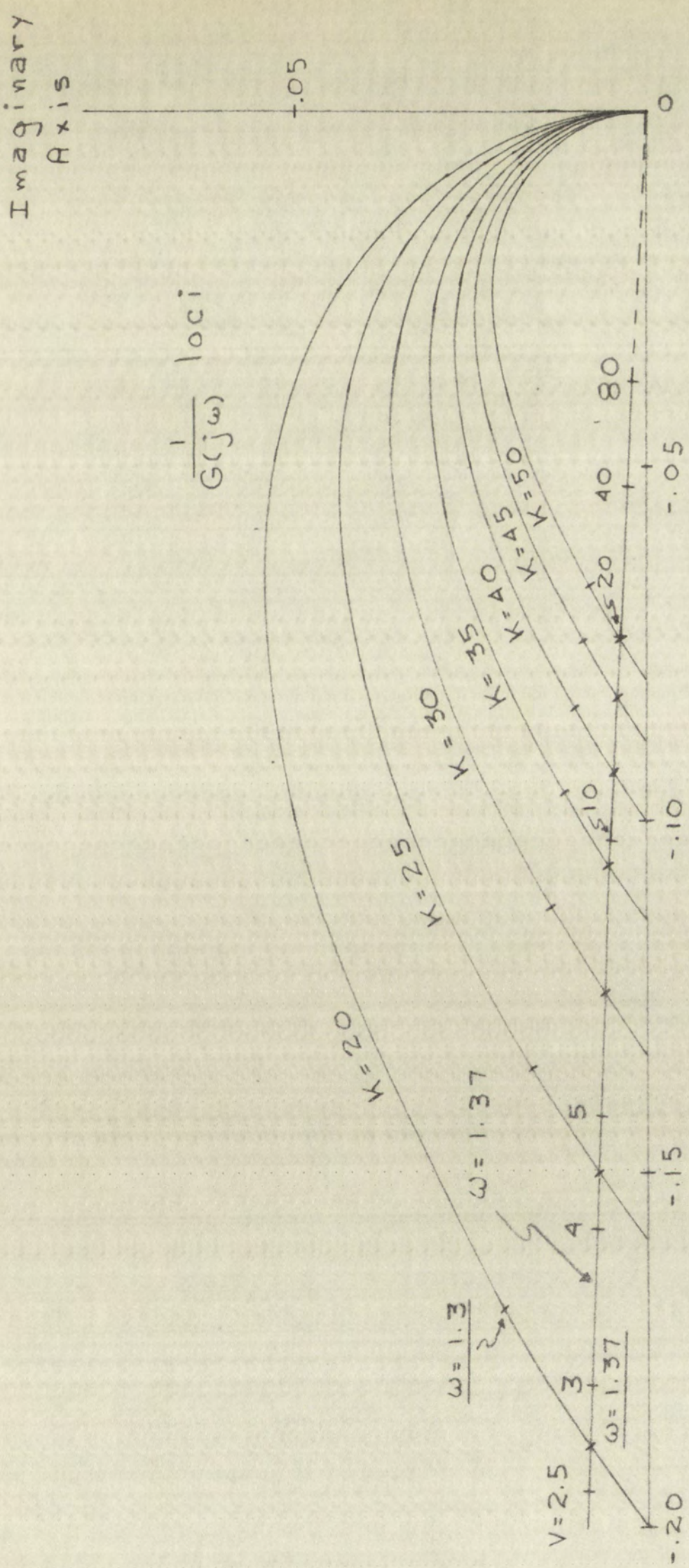

Figure 16.--Graphical determination of limit cycles for system A

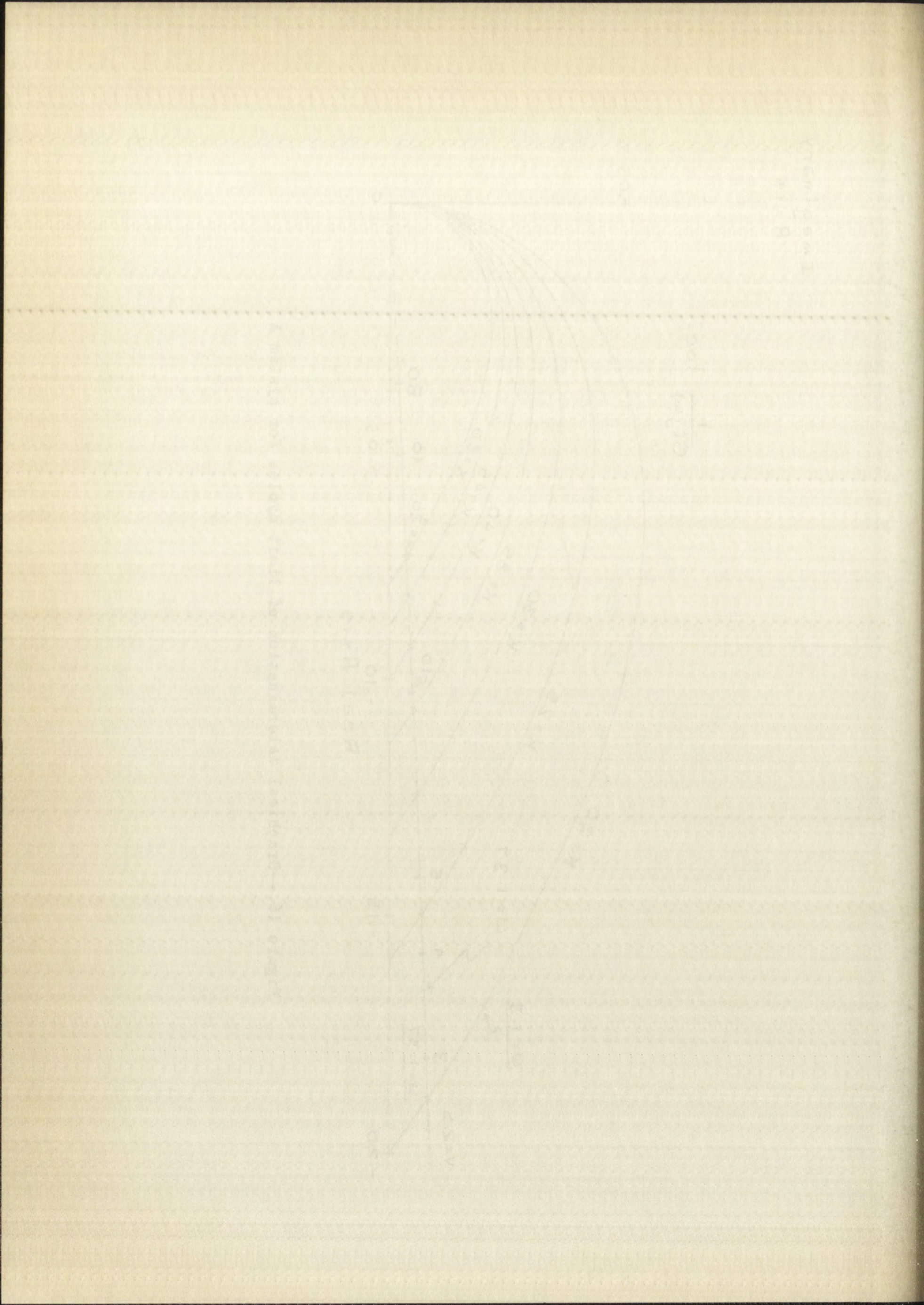

Figure 17 shows a polar plot of $1/G(j\omega)$ superimposed on a plot of $-N(V,\omega)$ for network B. For the value of gain used, K = 20, one equilibrium point is between ω = 0.3 and ω = 0.4 on the $1/G(j\omega)$ locus and the other point is in the vicinity of ω= 1.4. The low frequency equilibrium point is stable, and the high frequency one is unstable. The stable oscillation is more important and is discussed first.

TABLE 1.--Calculated limit cycles for system A

K	Amplitude	Frequency
20	2.75	1.37
25	4.45	1.37
30	6.60	1.37
35	9.20	1.37
40	12.5	1.37
45	15.8	1.37
50	19.5	1.37

Notes:

Amplitude is in volts.
Frequency is in radians per second.

The limit cycles for system B are found much the same as those for system A, except that the process is much more difficult, involving much trial and error. Table 2 gives the amplitudes and frequencies of the stable oscillation for system B for several values of gain.

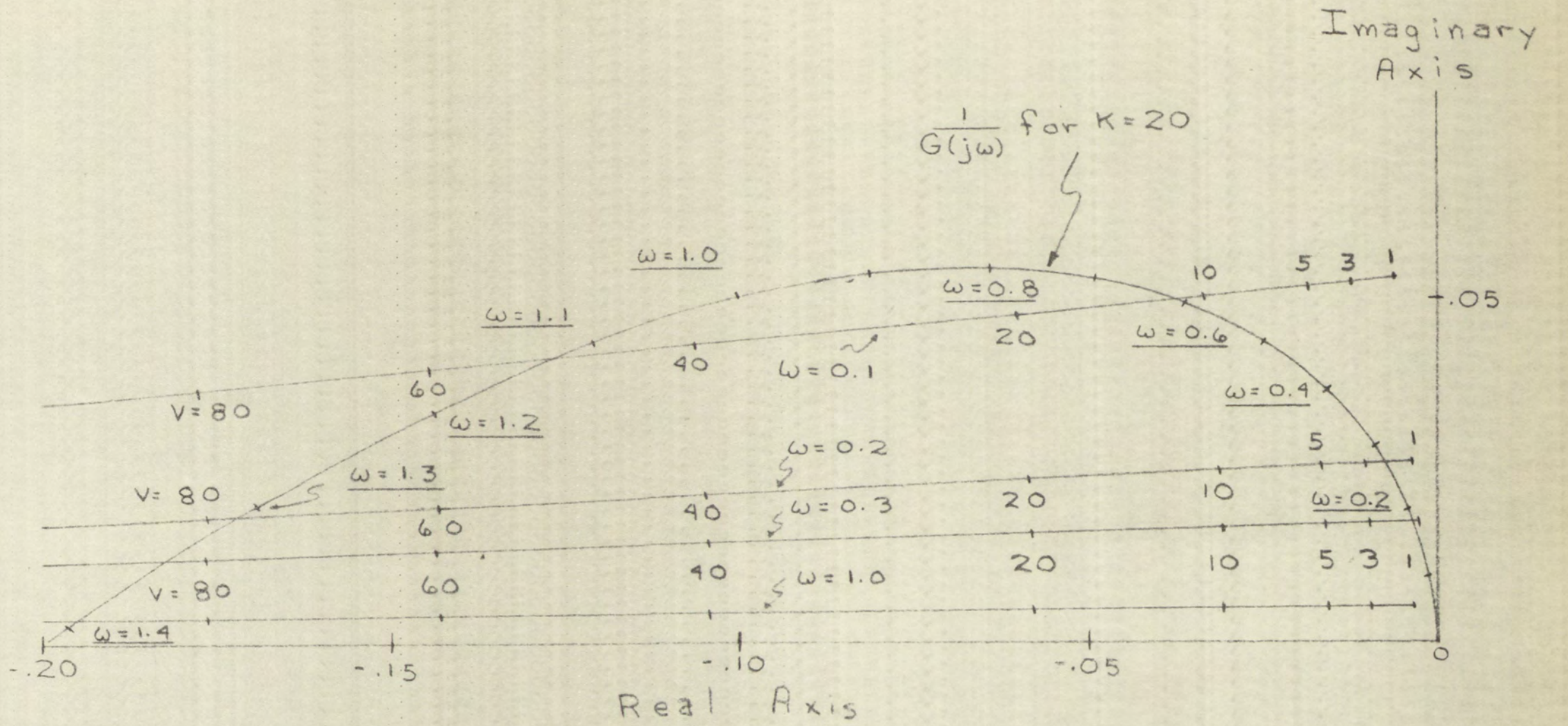

Figure 17.--Polar plot of describing function for network B

A brief examination of the unstable equilibrium point for at least one value of gain is of some interest here. In Figure 17 it is seen that for K = 20, the frequency of the unstable oscillation is ω = 1.4 radians per second. The amplitude is 94 volts. An examination of the loci shows that a slight decrease in amplitude results in the output settling down to the low frequency equilibrium point. A slight increase in amplitude causes the output to increase without bound. This indicates that if the error signal of the closed-loop system reaches an amplitude greater than 94 volts at a frequency of 1.4 radians per second, the system goes unstable. This point was also checked by means of computer simulation.

TABLE 2.--Calculated limit cycles for system B

K	Amplitude	Frequency
20	1.55	0.233
30	1.65	0.288
40	1.70	0.335
50	1.72	0.377

Notes:

Amplitude is in volts.
Frequency is in radians per second.

System C

Figure 18 is a polar plot of $-N(V,\omega)$ for network C superimposed on the $1/G(j\omega)$ locus for K = 20. The describing function loci for various values of ω coincide in the voltage and frequency

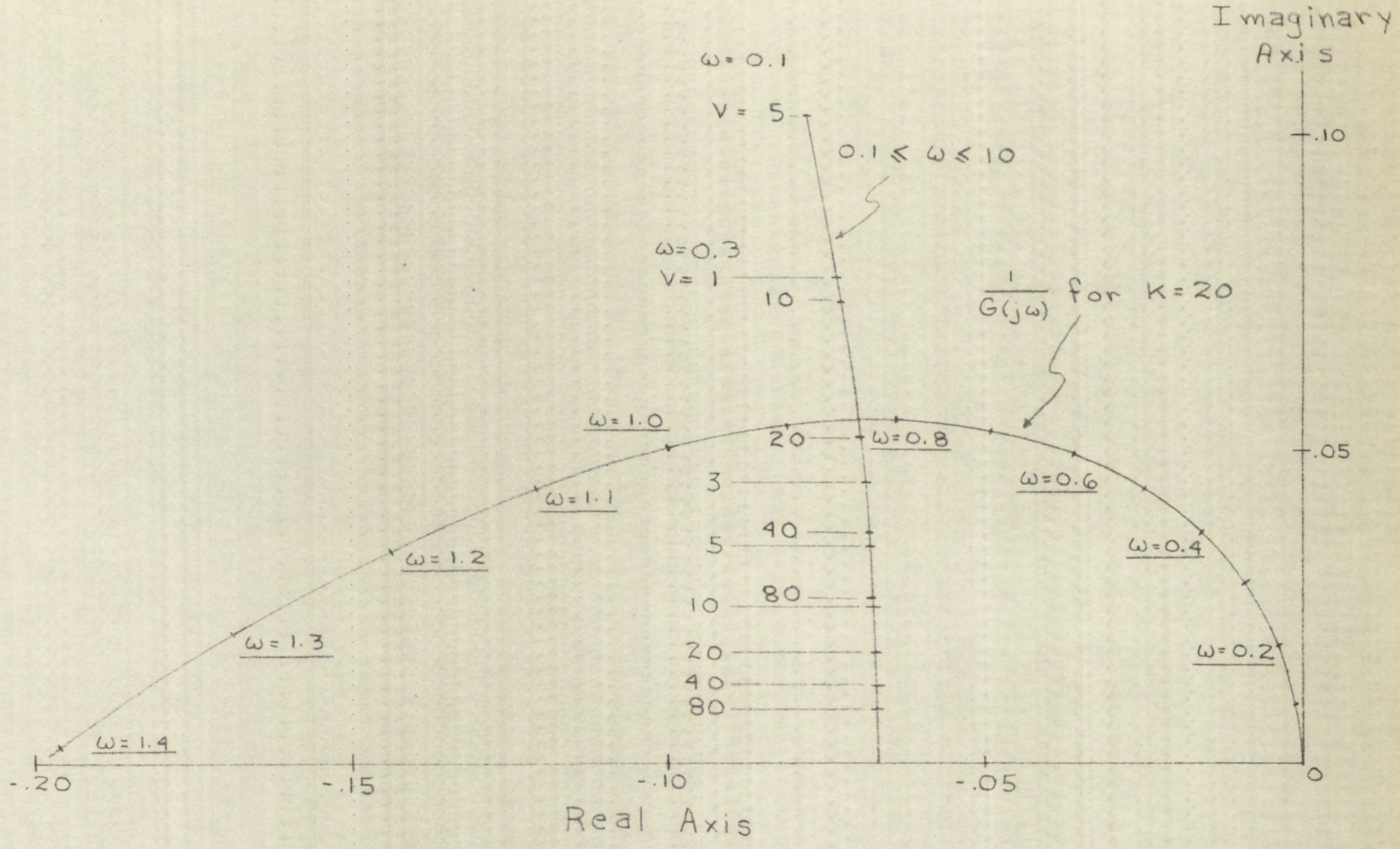

Figure 18.--Polar plot of describing function for network C

ranges of interest. The voltage corresponding to a particular point on the describing function curve depends on the frequency, of course. The voltage scales for several frequencies are shown on this curve.

In this case the frequency corresponding to the value of $1/G(j\omega)$ at the intersection of the two loci is the frequency of the sustained oscillation, which is stable. The amplitude may be found by calculating a describing function for each of these frequencies. The results of this procedure are given in Table 3.

TABLE 3.--Calculated limit cycles for system C

K	Amplitude	Frequency
20	0.261	0.837
30	0.486	1.01
40	1.120	1.16
50	4.28	1.29

Notes:

Amplitude is in volts.
Frequency is in radians per second.

III. STABILITY ANALYSIS BY COMPUTER SIMULATION

In addition to the theoretical analysis using the describing function approach, the question of stability was investigated by means of analog computer simulation. The actual computer setups which were used are discussed in Appendix C; only the results are given here.

System A

It was found that when network A is used as compensation for the closed-loop system, a limit cycle does occur, and that at least several types of disturbances excite the oscillation. Single pulses of varying amplitudes and step-function inputs were both used, and a limit cycle resulted in all cases.

The amplitudes and frequencies of the limit cycles which were obtained by computer simulation are given in Table 4. The values obtained by means of the describing function are also given for purposes of comparison.

TABLE 4.--Limit cycles for system A obtained by computer simulation compared with calculated limit cycles

K	Amplitude			Frequency		
	Simulation	Calculation	Difference	Simulation	Calculation	Difference
20	2.78	2.75	1.1%	1.37	1.37	-
25	4.32	4.45	3.0%	1.37	1.37	-
30	6.55	6.60	0.8%	1.37	1.37	-
35	9.10	9.20	1.1%	1.37	1.37	-
40	12.3	12.5	1.6%	1.37	1.37	-
45	15.5	15.8	1.9%	1.37	1.37	-
50	19.4	19.5	0.5%	1.37	1.37	-

Notes:

Amplitude is in volts. Frequency is in radians per second.

The agreement between the two sets of results is rather remarkable. It certainly indicates that the describing function

method is a reasonably accurate one in spite of the approximations which are made.

It is clear from both methods of analysis that the existence of a limit cycle is unavoidable, regardless of the gain and the magnitude of the input step.

System B

It was found that even a slight disturbance at the input caused this system to go into a stable limit cycle. In this case, however, the system became absolutely unstable if the disturbance was too large. This is discussed further below.

The amplitudes and frequencies of the stable oscillation for system B are given in Table 5. As before, the calculated results are also given.

TABLE 5.--Limit cycles for system B obtained by computer simulation compared with calculated limit cycles

K	Amplitude			Frequency		
	Simulation	Calculation	Difference	Simulation	Calculation	Difference
20	1.56	1.55	0.7%	0.233	0.233	-
30	1.65	1.65	-	0.284	0.288	1.4%
40	1.70	1.70	-	0.335	0.335	-
50	1.74	1.72	1.2%	0.375	0.377	0.6%

Notes:

Amplitude is in volts. Frequency is in radians per second.

Here again, the agreement between the two sets of results is

very encouraging.

It was found that the output of this system increases without bound if the magnitude of the input step is greater than a certain value. For K = 20, a step of 109 volts resulted in instability. The initial overshoot in this case was 90 volts; the frequency of the initial oscillation was 1.41 radians per second. These values compare favorably with those predicted by the describing function, 94 volts and 1.4 radians per second. The output for an input of 109u(t) is shown in Figure 19.

For K = 30, the system went unstable when r(t) = 62 u(t); for K = 40, r(t) = 42 u(t); and for K = 50, r(t) = 36 u(t).

System C

A stable sustained oscillation was found to exist for all values of gain between twenty and fifty. As with the other two systems, even a slight disturbance at the input caused the system to go into the limit cycle.

The amplitudes and frequencies of the limit cycles for several values of K are given in Table 6, page 33.

As with the other two systems, the agreement between the values obtained by simulation and by calculation is very good.

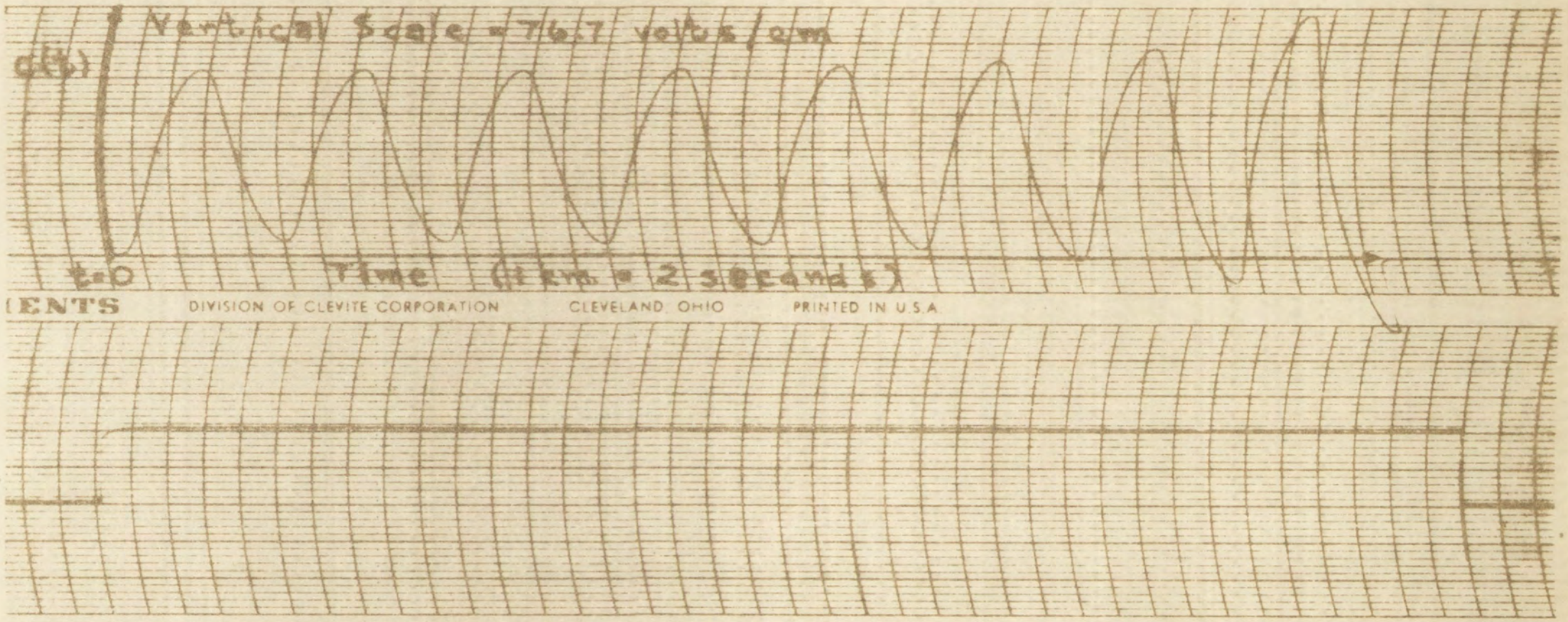

Figure 19.—Response of system B for K = 20, r(t) = 109 u(t)

TABLE 6.--Limit cycles for system C obtained by computer simulation compared with calculated limit cycles

K	Amplitude			Frequency		
	Simulation	Calculation	Difference	Simulation	Calculation	Difference
20	0.255	0.261	2.4%	0.839	0.837	0.2%
30	0.476	0.486	2.1%	1.01	1.01	-
40	1.11	1.12	0.9%	1.16	1.16	-
50	4.38	4.28	2.3%	1.30	1.29	0.8%

Notes:

Amplitude is in volts. Frequency is in radians per second.

CHAPTER III

STEP-FUNCTION RESPONSE

In addition to the investigation of the limit cycles of the nonlinear system by means of analog computer simulation, the step-function responses for each system were also found by this method. The results are discussed in this chapter.

I. SYSTEM A

The step-function responses for system A for K = 20 are shown in Figure 20. The response of the linear system resulting from the employment of the RC network in Figure 3, page 3, as compensation for the system in Figure 2, page 3, is given for purposes of comparison.

Each of the responses for the nonlinear system settled into a limit cycle. For the larger values of input, the amplitude deviated somewhat from that shown in Table 4, page 29, due to the inaccuracy of the simulation in these ranges. This is discussed further in Appendix C.

Figure 20 shows that the larger the amplitude of the input step, the smaller the overshoot and the slower the rise-time. A comparison with the response of the linear system indicates that there is certainly no improvement in the step-function response as a result of the insertion of the nonlinearity in the compensation network.

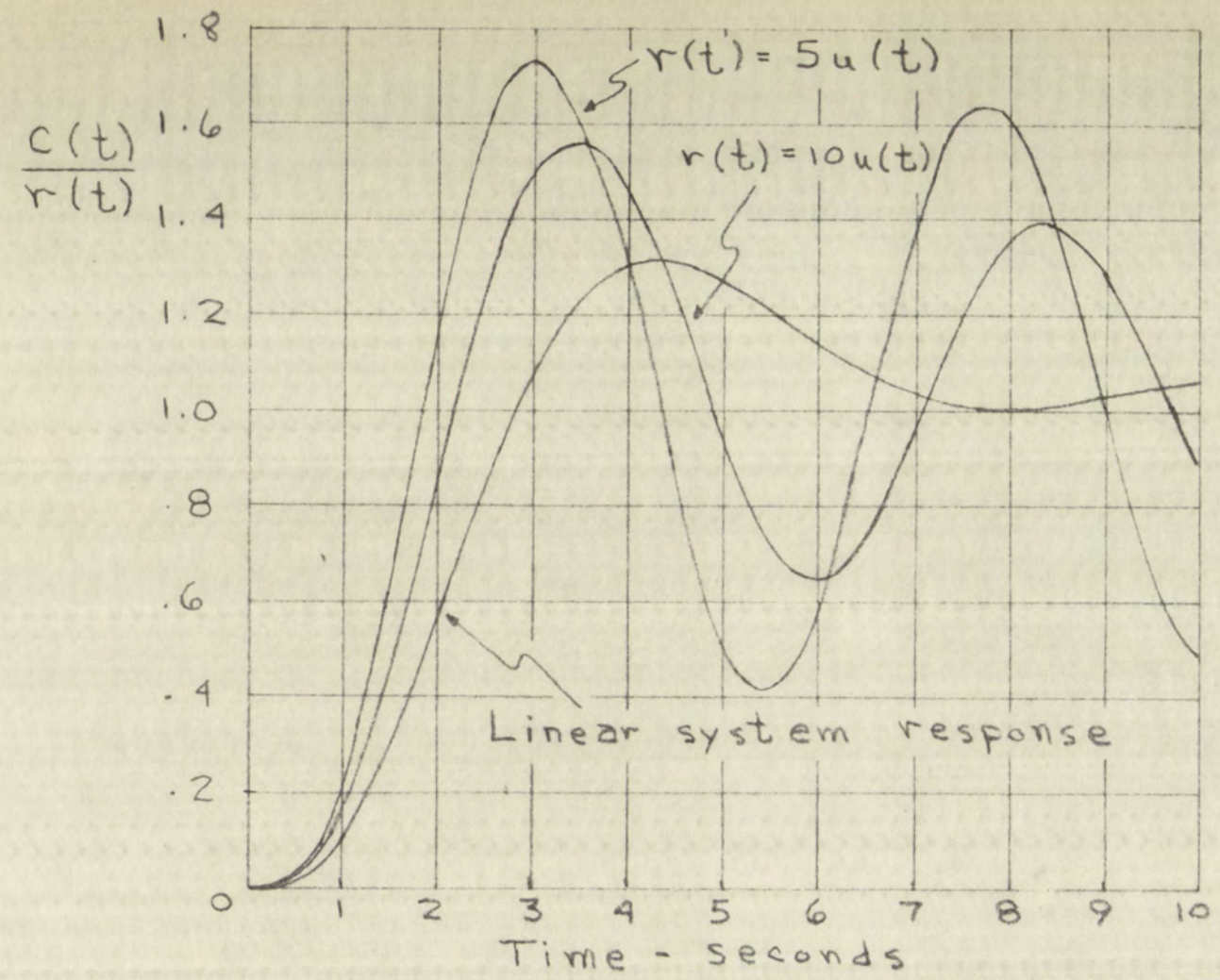

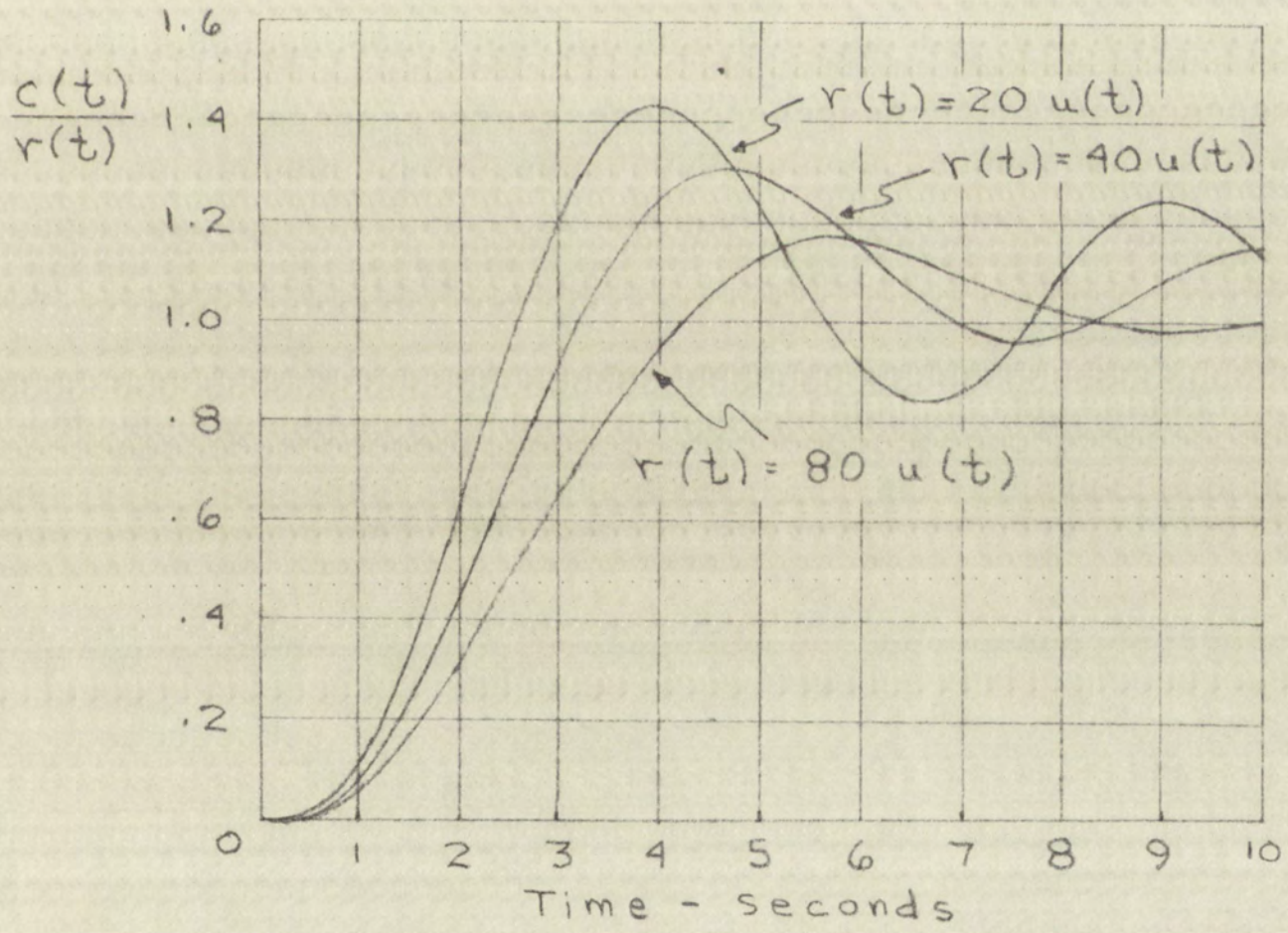

Figure 20.--Step-function responses of system A for K = 20

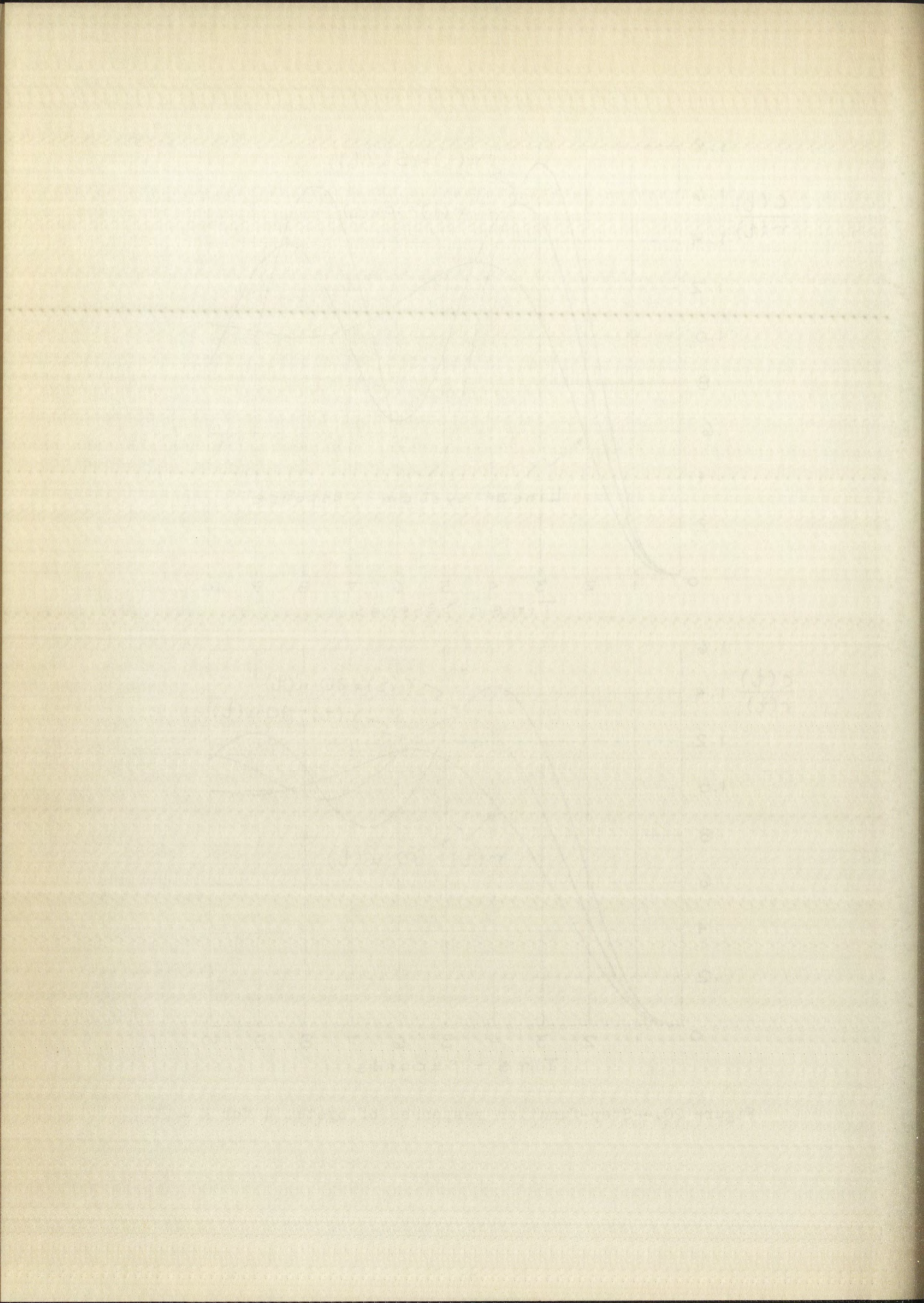

The responses were also found for several other values of open loop gain, specifically, K = 30, 40, and 50. As expected, increasing the gain increased the overshoot and the amplitude of the limit cycle. Except for this, the family of curves remained much the same as that shown in Figure 20. Of course, as the amplitude of the limit cycle became larger than the magnitude of the input step, the output voltage was negative at times. This was as expected.

II. SYSTEM B

The step-function responses for this system for K = 20 are shown in Figure 21. The step response of the linear system is also shown. Each of the nonlinear responses went into the limit cycle corresponding to a gain of twenty.

The responses for this system are rather unusual in that not only the overshoot and the rise-time vary with the magnitude of the input step, but the waveshape changes considerably, also. It should be noted that the overshoot does not vary monotonically with the magnitude of the input; as the magnitude is increased, the overshoot first decreases and then starts to increase again.

The responses show that as the magnitude of the step is increased, a high frequency component appears in the response. After a short time, this component disappears and the response settles down to the lower frequency limit cycle.

The responses for several other values of gain were found,

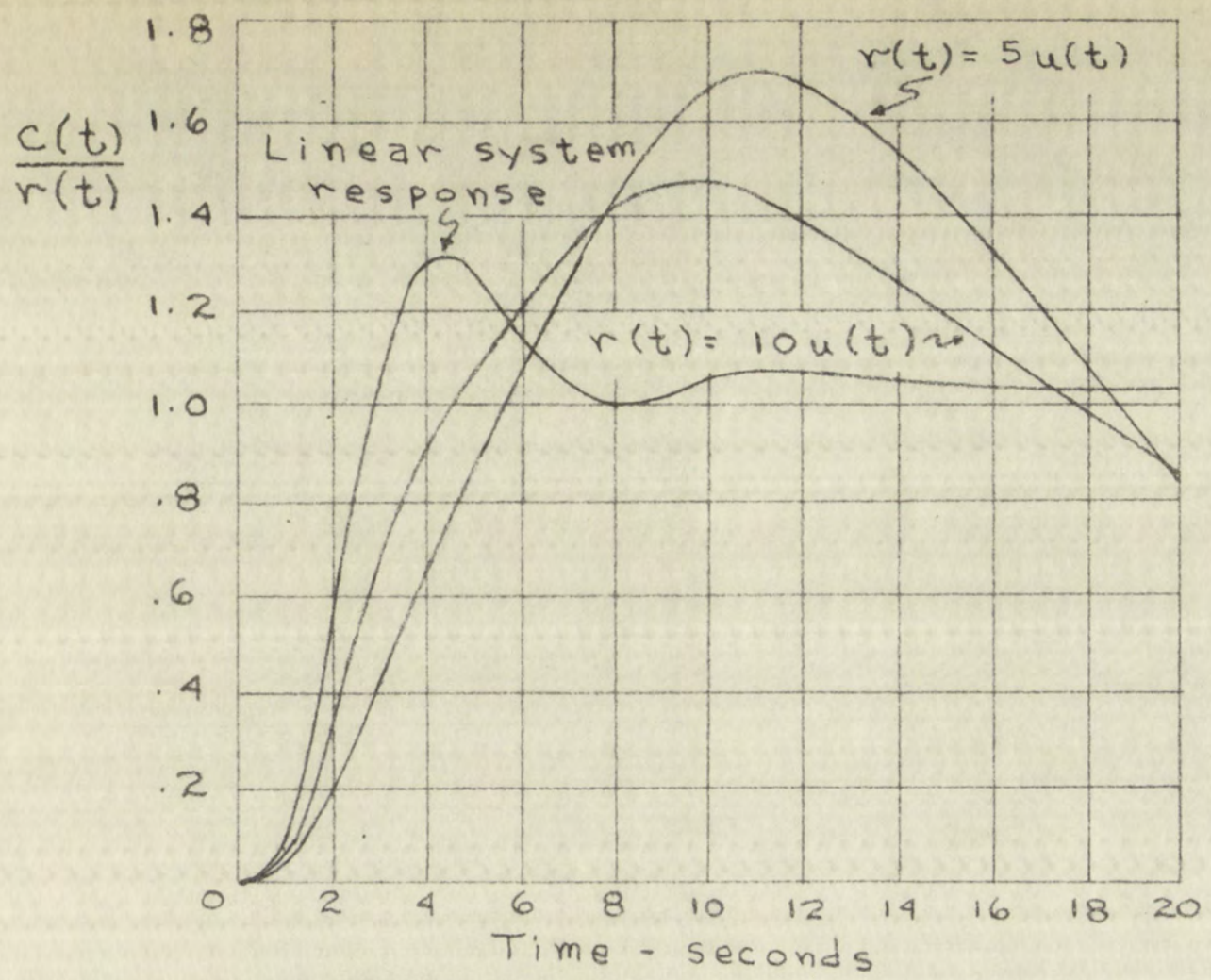

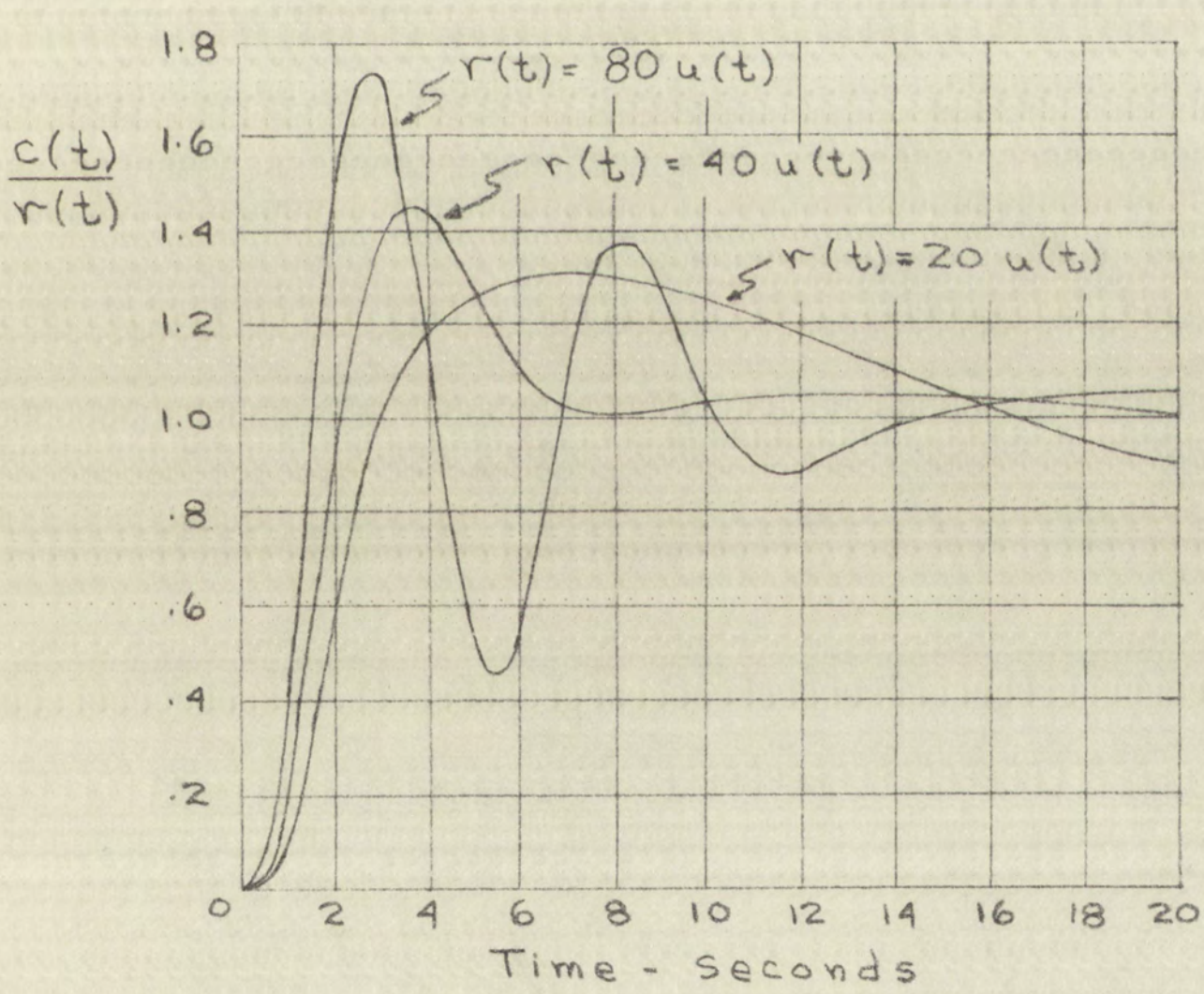

Figure 21.--Step-function responses of system B for K = 20

and the main effect noted was that as the gain was increased, the high frequency signal appeared for increasingly smaller inputs. For example, Figure 21 shows that for K = 20, the high frequency component is first evident for r(t) = 40 u(t). For a gain of K = 30, it appeared when r(t) = 20 u(t); for K = 50, r(t) = 10 u(t). The decay time of the high frequency oscillation also increased with the gain.

As mentioned in the second chapter, this system went absolutely unstable as the magnitude of the input step exceeded a certain value.

III. SYSTEM C

The step-function responses for this system when K = 20 are shown in Figure 22. Each of the responses eventually settled into a limit cycle, although some deviation in the amplitude was observed. This deviation was due to inaccuracies in the simulation for large values of input.

It is interesting to note that in this case, changing the magnitude of the input step had very little effect on the rise-time of the response; it affected only the overshoot. Comparison with the linear response indicates that the rise time of the linear and nonlinear responses are about the same.

Another interesting comparison can be made between the linear response and the nonlinear response for r(t) = 20 u(t). Examination of Figure 22 shows that they have almost identical rise times and

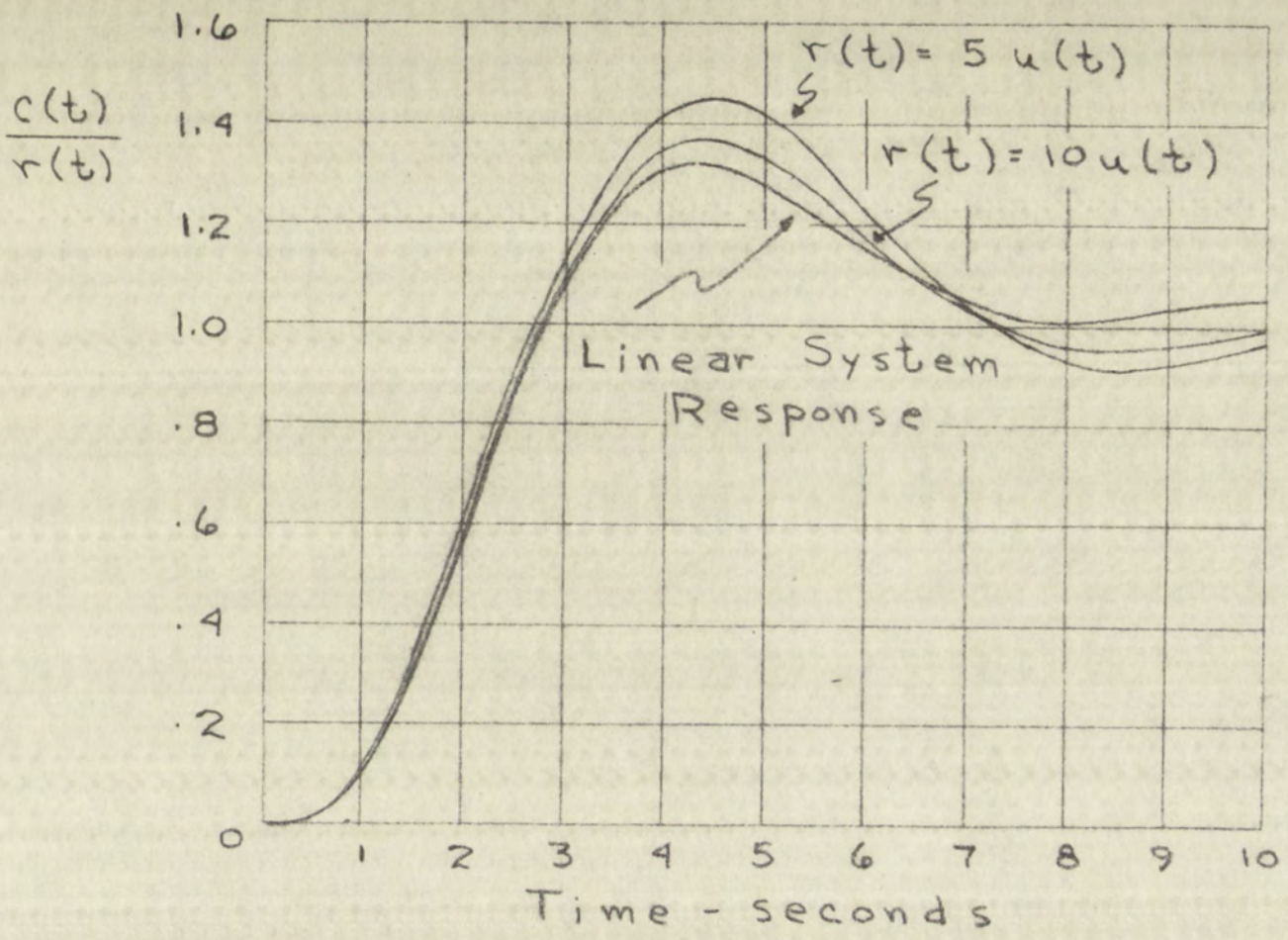

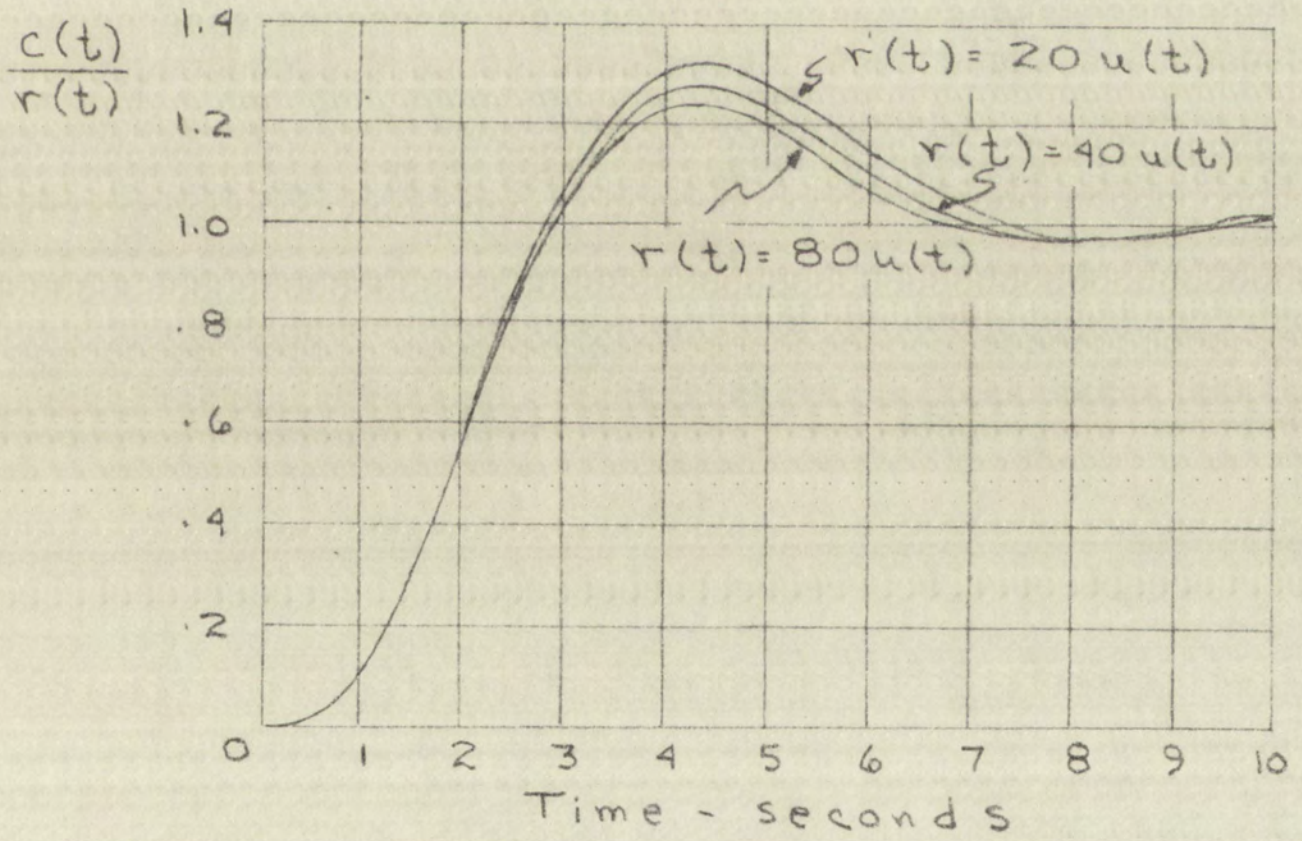

Figure 22.--Step-function responses of system C for K = 20

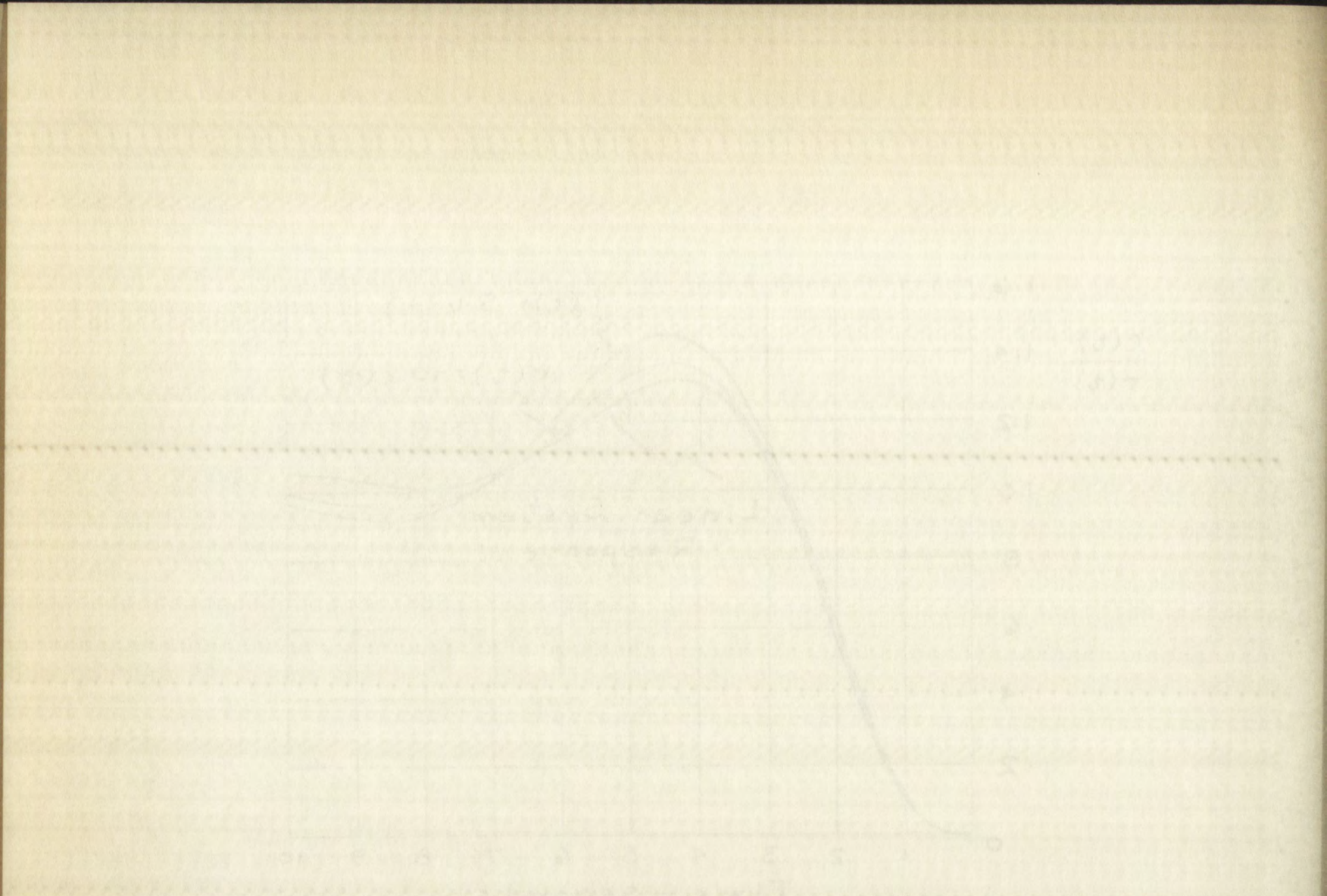

overshoots.

This fact acquires more significance when it is recalled that k_1 and k_2 were chosen so that for a current of one microampere, the d-c resistance of each nonlinear element is the same as that of the corresponding linear element.

If a twenty-volt step is applied to the compensation network, the initial current is one microampere. Hence, when a twenty-volt step is used as the input to the closed-loop system, the nonlinear network and the linear one appear about the same for a short time after zero. While it is dangerous to carry this line of reasoning too far, the fact is certainly worthy of note.

The step-function responses were found for K = 30, 40, and 50; and the effects which were observed were not unexpected. As the gain was increased, the overshoot increased and the rise-time decreased. The amplitude of the limit cycle increased. Except for these differences, the relationships of the responses for the various input steps remained about the same as in Figure 22.

CHAPTER IV

SUMMARY AND CONCLUSIONS

The general aim of this thesis was to study the effect of a nonlinear compensation network on the closed-loop response of a feedback control system. The detrimental effects of such an insertion were investigated, and the possibility of improving the system was studied.

Three different nonlinear networks were considered in a specific control system. Both the stability and the step-function response of each of the resulting systems were studied.

It was found by both the describing function method and by computer simulation that all three of the nonlinear systems go into limit cycles. The amplitudes and frequencies of these sustained oscillations were found by both methods, and the two sets of results agreed quite well.

When network B was used for compensation, the system was driven into absolute instability by using sufficiently large inputs.

The step-function responses when networks A and B were used as compensation showed no improvement over the linear system; and for certain ranges of input, the response was much worse.

It was found that the use of network C results in some improvement in the step-function response for certain ranges of operation. Even outside these ranges, the performance was not

markedly different from that of the linear system. This is of interest because network C is more likely to occur in practice than the other two networks.

Thus, there was no general improvement in performance for any of the three systems. It was noted, however, that the detrimental effects on system performance caused by using network C are not very great, especially if a small limit cycle can be tolerated. Whether this system would be satisfactory for a specific situation depends on the requirements of the problem.

BIBLIOGRAPHY

BIBLIOGRAPHY

Bower, John L. and Peter M. Schultheiss. Introduction to the Design of Servomechanisms. New York: John Wiley and Sons, Inc., 1958. 510 pp.

Bruns, Robert A. and Robert M. Saunders. Analysis of Feedback Control Systems. New York: McGraw-Hill Book Company, Inc., 1955. 383 pp.

Chestnut, Harold and Robert W. Mayer. Servomechanisms and Regulating System Design. 2 vols. New York: John Wiley and Sons, Inc., 1955-1959.

Cosgriff, Robert Lien. Nonlinear Control Systems. New York: McGraw-Hill Book Company, Inc., 1958. 328 pp.

D'Azzo, John J. and Constantine H. Houpis. Feedback Control System Analysis and Synthesis. New York: McGraw-Hill Book Company, Inc., 1960. 580 pp.

Fett, Gilbert Howard. Feedback Control Systems. Englewood Cliffs, New Jersey: Prentice-Hall, Inc., 1954. 361 pp.

Gille, J-C, M. J. Pélegrin, and P. Decaulne. Feedback Control Systems. New York: McGraw-Hill Book Company, Inc., 1959. 793 pp.

Johnson, Clarence L. Analog Computer Techniques. New York: McGraw-Hill Book Company, Inc., 1956. 264 pp.

Kochenburger, R. J. "A Frequency Response Method for Analyzing and Synthesizing Contactor Servomechanisms," Transactions of the A.I.E.E.-Part I, LXIX (1950), 270-284.

Ku, Y. H. Analysis and Control of Nonlinear Systems. New York: The Ronald Press Company, Inc., 1958. 360 pp.

Mishkin, Eli and Ludwig Braun, Jr. (ed.). Adaptive Control Systems. New York: McGraw-Hill Book Company, Inc., 1961. 533 pp.

Murphy, Gordon J. Control Engineering. New York: D. Van Nostrand Company, Inc., 1959. 385 pp.

Savant, C. J., Jr. Basic Feedback Control System Design. New York: McGraw-Hill Book Company, Inc., 1958. 418 pp.

Thaler, George J. Elements of Servomechanism Theory. New York: McGraw-Hill Book Company, Inc., 1955. 282 pp.

Truxal, John G. Automatic Feedback Control System Synthesis. New York: McGraw-Hill Book Company, Inc., 1955. 675 pp.

APPENDIX

APPENDIX A

EFFECT OF CHANGING THE NONLINEAR PARAMETERS, k_1 AND k_2

Throughout the preceding discussion, one set of values has been used for the nonlinear parameters, k_1 and k_2. This has simplified the various calculations and also the presentation of data. It is appropriate, however, to investigate the possibility of extending the results which were obtained to compensation networks with other values of k_1 and k_2.

The specific problem to be considered here is this: if the nonlinear paramter or parameters in one of the three networks are multiplied by some positive constant M, and the input voltage is multiplied by 1/M, what is the effect on the current and on the output voltage? Each of the three circuits shown in Figure 4, page 5, is considered separately. The effect on the closed-loop system is also discussed.

Network A

Consider the network shown in Figure 23. For each $v_1(t)$, there exist an $i(t)$ and a $v_2(t)$ such that

$$v_1(t) = k_1\, i(t)\,|i(t)| + R_2\, i(t) + \frac{1}{C}\int i(t)\,dt \qquad (A.1)$$

and

$$v_2(t) = R_2\, i(t) + \frac{1}{C}\int i(t)\,dt \qquad (A.2)$$

Consider now the network shown in Figure 24. If $v_1^*(t)$ =

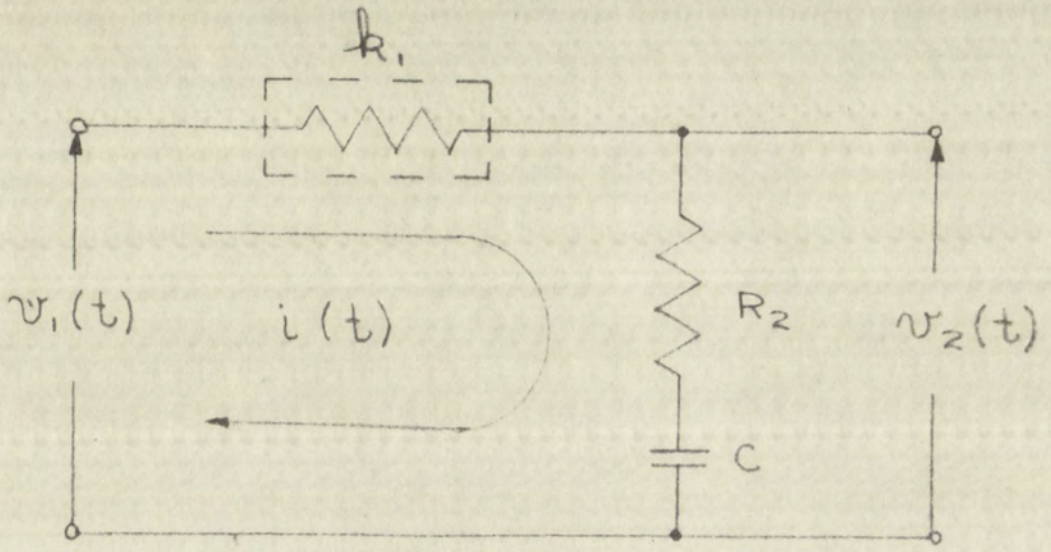

Figure 23.--Network A with nonlinear resistance k_1

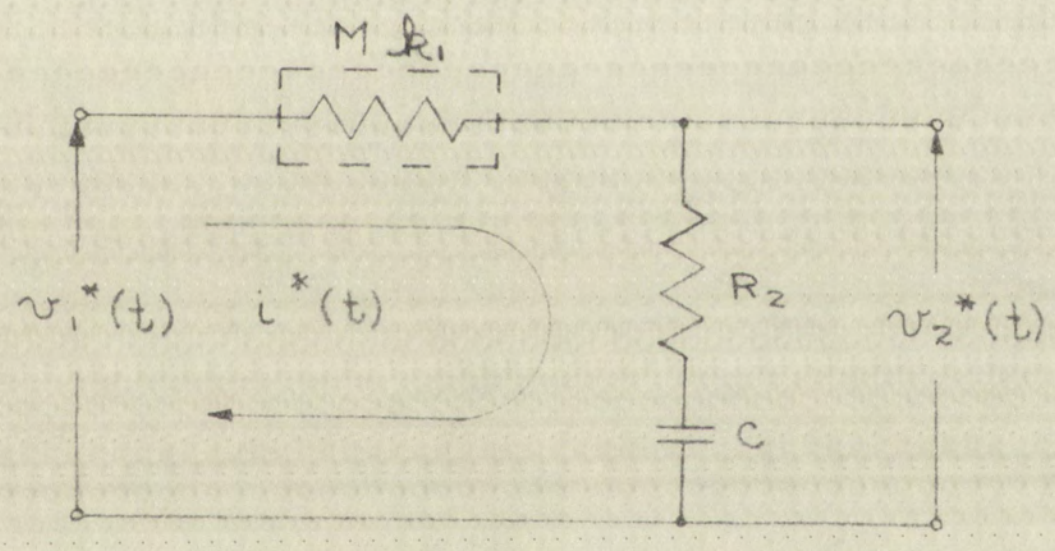

Figure 24.--Network A with nonlinear resistance Mk_1

$v_1(t)/M$, it is of interest to ascertain whether $i^*(t)$ and $v_2^*(t)$ bear any relation to $i(t)$ and $v_2(t)$, where $v_1(t)$, $i(t)$, and $v_2(t)$ are the same functions as those in Figure 23. This can be done by examining the differential equation which $i^*(t)$ must satisfy.

$$\frac{v_1(t)}{M} = M k_1 \left[i^*(t) \left| i^*(t) \right| \right] + R_2 i^*(t) + \frac{1}{C} \int i^*(t)\, dt \qquad \text{(A.3)}$$

Multiplying both sides by M,

$$v_1(t) = k_1 \left[M i^*(t) \left| M i^*(t) \right| \right] + R_2 M i^*(t)$$

$$+ \frac{1}{C} \int M i^*(t)\, dt \qquad \text{(A.4)}$$

Examination of equation (A.1) indicates that $i^*(t) = i(t)/M$ is a solution to equation (A.4). Hence,

$$v_2^*(t) = R_2 \frac{i(t)}{M} + \frac{1}{C} \int \frac{i(t)}{M} dt = \frac{v_2(t)}{M} \qquad \text{(A.5)}$$

Network B

Next, the network shown in Figure 25 is considered. As before, for every $v_1(t)$, there exist an $i(t)$ and a $v_2(t)$ such that

$$v_1(t) = R_1 i(t) + k_2 i(t) \left| i(t) \right| + \frac{1}{C} \int i(t)\, dt \qquad \text{(A.6)}$$

and $$v_2(t) = k_2 i(t) \left| i(t) \right| + \frac{1}{C} \int i(t)\, dt \qquad \text{(A.7)}$$

Now consider the network shown in Figure 26. As above, if $v_1^*(t) = v_1(t)/M$, it is desirable to investigate the relationship between $i^*(t)$ and $i(t)$ and $v_2^*(t)$ and $v_2(t)$. As before, the

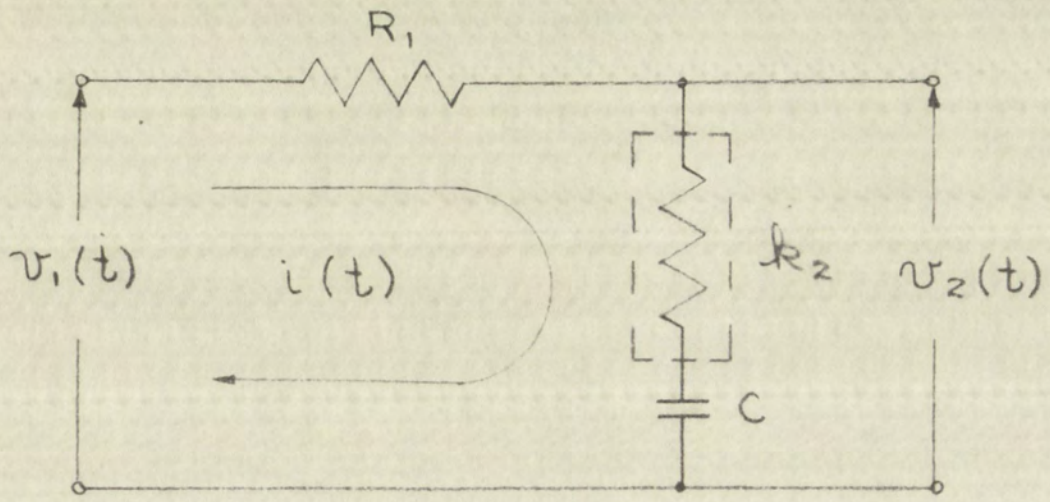

Figure 25.--Network B with nonlinear resistance k_2

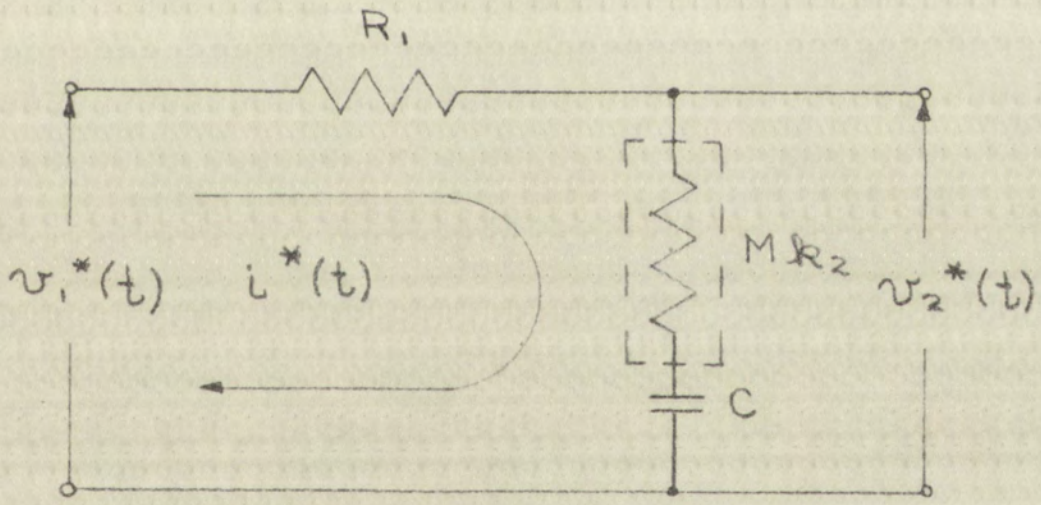

Figure 26.--Network B with nonlinear resistance Mk_2

differential equation which i*(t) must satisfy is written.

$$\frac{v_1(t)}{M} = R_1 i^*(t) + M k_2 i^*(t)|i^*(t)| + \frac{1}{C}\int i^*(t)\,dt \quad \text{(A.8)}$$

Multiplying both sides by M,

$$v_1(t) = R_1 M i^*(t) + k_2\left[M i^*(t)\,|M i^*(t)|\right]$$

$$+ \frac{1}{C}\int M i^*(t)\,dt \quad \text{(A.9)}$$

From equation (A.6) it is seen that $i^*(t) = i(t)/M$ is a solution to equation (A.9). Consequently,

$$v_2^*(t) = M k_2 \frac{i(t)}{M}\left|\frac{i(t)}{M}\right| + \frac{1}{C}\int \frac{i(t)}{M}\,dt$$

$$= \frac{v_2(t)}{M} \quad \text{(A.10)}$$

Network C

This circuit is shown in Figure 27. For every $v_1(t)$, there exist an i(t) and a $v_2(t)$ such that

$$v_1(t) = (k_1 + k_2)\left[i(t)|i(t)|\right] + \frac{1}{C}\int i(t)\,dt \quad \text{(A.11)}$$

and

$$v_2(t) = k_2\left[i(t)|i(t)|\right] + \frac{1}{C}\int i(t)\,dt \quad \text{(A.12)}$$

The network shown in Figure 28 is now considered. If $v_1^*(t) = v_1(t)/M$, then i*(t) must satisfy the differential equation

$$\frac{v_1(t)}{M} = M(k_1 + k_2)\left[i^*(t)|i^*(t)|\right] + \frac{1}{C}\int i^*(t)\,dt \quad \text{(A.13)}$$

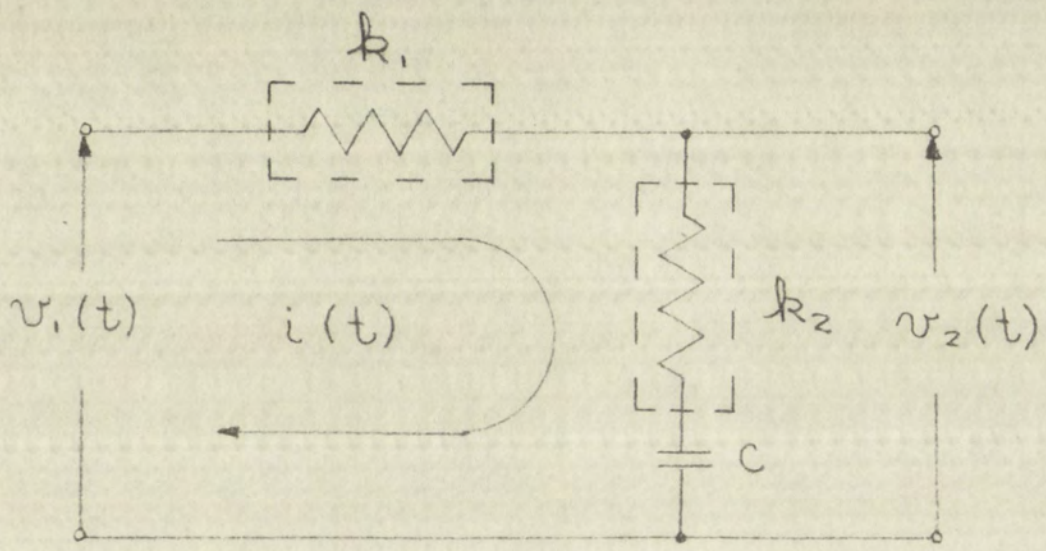

Figure 27.--Network C with nonlinear resistances k_1 and k_2

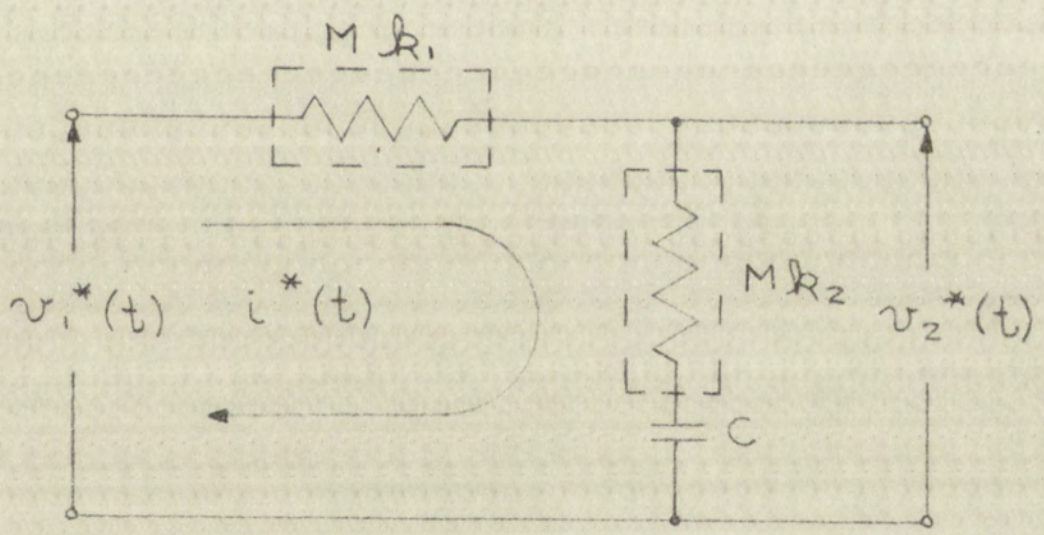

Figure 28.--Network C with nonlinear resistances Mk_1 and Mk_2

Multiplying both sides by M,

$$v_1(t) = (k_1 + k_2)\left[M i^*(t) \left| M i^*(t) \right|\right] + \frac{1}{C}\int M i^*(t)\, dt \quad \text{(A.14)}$$

An examination of equation (A.11) reveals that $i^*(t) = i(t)/M$ is a solution to equation (A.14). Hence,

$$v_2^*(t) = M k_2 \frac{i(t)}{M}\left|\frac{i(t)}{M}\right| + \frac{1}{C}\int \frac{i(t)}{M}\, dt$$

$$= \frac{v_2(t)}{M} \quad \text{(A.15)}$$

With these results in mind, it is possible to make a general statement which applies to all three networks. Assume that for an input $v_1(t)$, the output is $v_2(t)$, and that the nonlinear resistances have values k_1, k_2, or k_1 and k_2. Then if a voltage $v_1(t)/M$ is applied to the corresponding network with parameters Mk_1, Mk_2, or Mk_1 and Mk_2, the output voltage is $v_2(t)/M$.

As might be expected, this result can be extended to a closed-loop system with one of the nonlinear networks used as a compensation network.

Closed-loop system

Consider the control system shown in Figure 29, page 55. G(s) may be any linear transfer function, and n is one of the networks shown in Figure 4, page 5. Corresponding to every r(t), there is a certain c(t). The following equations may be written.

$$\mathcal{L}[c(t)] = C(s) = V_2(s)G(s) = \mathcal{L}[v_2(t)]\,G(s) \quad \text{(A.16)}$$

$$v_1(t) = r(t) - c(t) \qquad \text{(A.17)}$$

In the system shown in Figure 30, n* is the same network as n in Figure 29 except that the nonlinear resistance parameter or parameters have been multiplied by a positive constant M. It can be shown that if $r^*(t) = r(t)/M$, then $c^*(t) = c(t)/M$. It is done by assuming that this is true and then examining the conditions which are implied to see if they are met.

If $c^*(t) = c(t)/M$, this requires that $v_2^*(t) = v_2(t)/M$ by equation (A.16). It was shown that this is true if $v_1^*(t) = v_1(t)/M$. But if $r^*(t) = r(t)/M$ and $c^*(t) = c(t)/M$, then $v_1^*(t) = r^*(t) - c^*(t) = \left[r(t) - c(t)\right]/M = v_1(t)/M$. Thus, the assumption that $c^*(t) = c(t)/M$ was correct.

Conclusions

These results lead to several conclusions. Suppose that for an input voltage V sin ω t, the describing function for one of the networks is $|N| \angle\beta$. Then for the corresponding circuit with the nonlinear parameter or parameters multiplied by M, the describing function for an input (V/M) sin ω t is also $|N| \angle\beta$.

Similarly, multiplying the parameters by M has the effect of multiplying the amplitude of the limit cycle corresponding to each value of K by 1/M. Their frequencies remain the same.

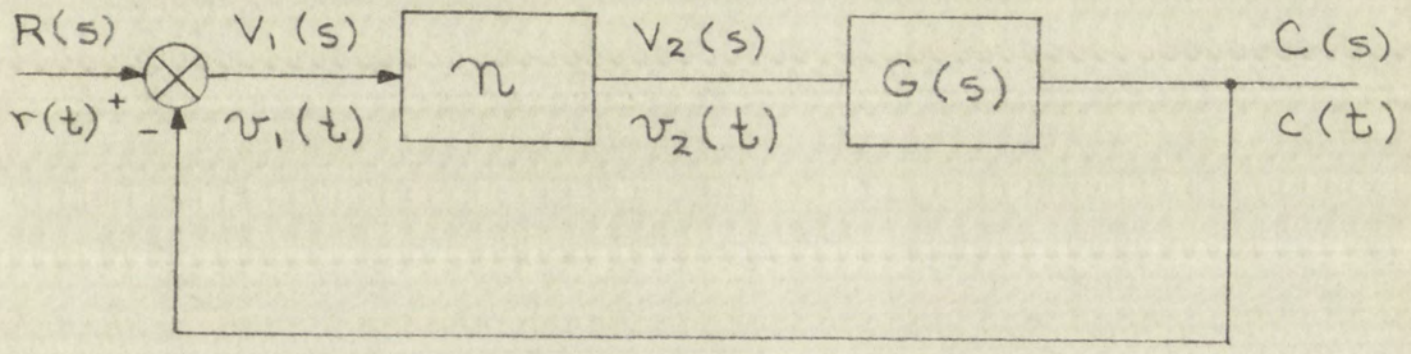

Figure 29.--Closed-loop system with nonlinear resistances k_1, k_2, or k_1 and k_2

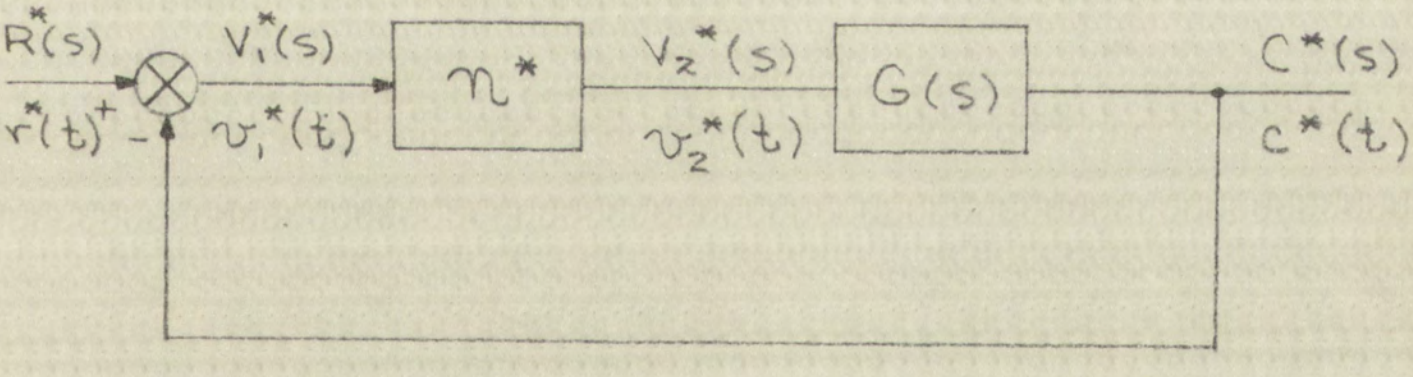

Figure 30.--Closed-loop system with nonlinear resistances Mk_1, Mk_2, or Mk_1 and Mk_2

APPENDIX B

COMPUTATION OF THE DESCRIBING FUNCTIONS

In the second chapter the describing functions for each of the three networks were presented in graphical form. The method of finding these describing functions is discussed in this appendix, and the results are presented in tabular form.

Network A

Reference is made to Figure 4, page 5, for a schematic of this network. An input voltage of the form

$$v_1(t) = V \sin(\omega t - \theta) \qquad (B.1)$$

is assumed, where V and ω are known and θ is to be calculated. This unknown phase shift is inserted in the input voltage for the sake of convenience.

The equations for the network with the assumed input voltage are:

$$V \sin(\omega t - \theta) = k_1 i|i| + R_2 i + \frac{1}{C}\int i\,dt \qquad (B.2)$$

and

$$v_2(t) = R_2 i + \frac{1}{C}\int i\,dt \qquad (B.3)$$

After steady state is established, the current, denoted by i_{ss}, has the form

$$i_{ss} = C_1 \sin \omega t + \sum_{m=2}^{\infty} C_m \sin(\omega t + \theta_m) \qquad (B.4)$$

No phase shift is needed in the fundamental term because of the θ which was assumed in $v_1(t)$.

The fundamental component of the steady state output voltage, v_{2ss} is then given by

$$v_{2ss} = R_2 C_1 \sin \omega t + \frac{1}{\omega C} C_1 \sin(\omega t - 90^\circ) \quad (B.5)$$

$$= C_1 \sqrt{R_2^2 + \left(\frac{1}{\omega C}\right)^2} \sin(\omega t - \cot^{-1} \omega RC) \quad (B.6)$$

$$= V_2 \sin(\omega t - \phi) \quad (B.7)$$

The describing function is simply

$$N(V, \omega) = \frac{V_2}{V} \angle \theta - \phi = |N| \angle \beta \quad (B.8)$$

Thus, in order to calculate the describing function, C_1 and θ must be found for various values of V and ω. Finding the exact solutions for these parameters is a rather formidable problem indeed; therefore, approximate methods must be used if the describing function is to be found with a reasonable amount of computational labor.

An examination of the network parameters shows that the voltage drop across the nonlinear element is larger than the drop across either of the other two elements for all but very small values of ω and i. Hence, it was assumed that in the steady state,

$$i_{ss}|i_{ss}| = I^2 \sin \omega t \quad (B.9)$$

The Fourier series for i_{ss} is then

$$i_{ss} = I(b_1 \sin \omega t + b_3 \sin 3\omega t + b_5 \sin 5\omega t + \cdots) \qquad (B.10)$$

where

$$b_1 = \frac{4}{\pi}\int_0^{\pi/2}\sqrt{\sin \omega t}\, \sin \omega t\, d(\omega t)$$

$$= \frac{4}{\pi}\int_0^{\pi/2} \sin^{3/2} x\, dx = \frac{4}{\pi}\left[\frac{\sqrt{\pi}}{2}\,\frac{\Gamma(1.25)}{\Gamma(1.75)}\right]$$

$$= \frac{2}{\sqrt{\pi}}\,\frac{\Gamma(1.25)}{\Gamma(1.75)} \qquad (B.11)$$

$$b_3 = \frac{4}{\pi}\int_0^{\pi/2}\sqrt{\sin \omega t}\, \sin 3\omega t\, d(\omega t)$$

$$= \frac{4}{\pi}\int_0^{\pi/2}(3 \sin^{3/2} x - 4 \sin^{7/2} x)\, dx$$

$$= \frac{1}{7}\,\frac{2}{\sqrt{\pi}}\,\frac{\Gamma(1.25)}{\Gamma(1.75)} \qquad (B.12)$$

$$b_5 = \frac{4}{\pi}\int_0^{\pi/2}\sqrt{\sin \omega t}\, \sin 5\omega t\, d(\omega t)$$

$$= \frac{4}{\pi}\int_0^{\pi/2}(5 \sin^{3/2} x - 20 \sin^{5/2} x + 16 \sin^{11/2} x)\, dx$$

$$= \frac{5}{77}\,\frac{2}{\sqrt{\pi}}\,\frac{\Gamma(1.25)}{\Gamma(1.75)} \qquad (B.13)$$

Other coefficients may be found by a similar process. Thus,

$$i_{ss} = \frac{2}{\sqrt{\pi}} \frac{\Gamma(1.25)}{\Gamma(1.75)} \left(\sin \omega t + \frac{1}{7} \sin 3\omega t + \frac{5}{77} \sin 5\omega t + \cdots\right) I \qquad (B.14)$$

Neglecting all but the fundamental term,

$$V \sin(\omega t - \theta) = k_1 I^2 \sin \omega t + \frac{2}{\sqrt{\pi}} \frac{\Gamma(1.25)}{\Gamma(1.75)} I \left(R_2 \sin \omega t - \frac{\cos \omega t}{\omega C}\right) \qquad (B.15)$$

This leads to the equations:

$$V = \sqrt{\left[k_1 I^2 + \frac{2}{\sqrt{\pi}} \frac{\Gamma(1.25)}{\Gamma(1.75)} R_2 I\right]^2 + \left[\frac{2}{\sqrt{\pi}} \frac{\Gamma(1.25)}{\Gamma(1.75)} \frac{I}{\omega C}\right]^2} \qquad (B.16)$$

and $$\theta = \cot^{-1}\left[\omega C k_1 I \frac{\sqrt{\pi}}{2} \frac{\Gamma(1.75)}{\Gamma(1.25)} + \omega R_2 C\right] . \qquad (B.17)$$

Equation (B.16) becomes

$$I^4 + \frac{2.22567156 R_2}{k_1} I^3 + \frac{1.1238403473}{k_1^2} \left[R_2^2 + \left(\frac{1}{\omega C}\right)^2\right] I^2 - \frac{V_1^2}{k_1^2} = 0 \qquad (B.18)$$

Values of k_1, R_2, and C are inserted and the equation is solved for various combinations of ω and V.

Then,

$$v_{2ss} = \frac{2}{\sqrt{\pi}} \frac{\Gamma(1.25)}{\Gamma(1.75)} I \left(R_2 \sin \omega t - \frac{\cos \omega t}{\omega C}\right) \qquad (B.19)$$

$$v_{2ss} = V_2 \sin(\omega t - \phi) \tag{B.20}$$

where

$$V_2 = \frac{2}{\sqrt{\pi}} \frac{\Gamma(1.25)}{\Gamma(1.75)} I \sqrt{R_2^2 + \left(\frac{1}{\omega C}\right)^2} \tag{B.21}$$

and

$$\phi = \cot^{-1}(\omega R_2 C) \tag{B.22}$$

The describing function is then found by equation (B.8).

Table 7 gives the results of this derivation.

Network B

This network is shown in Figure 4, page 5. As for network A, an input voltage of the form

$$v_1(t) = V \sin(\omega t - \Theta) \tag{B.23}$$

is assumed. Then,

$$V \sin(\omega t - \Theta) = R_1 i + k_2 i|i| + \frac{1}{C}\int i\,dt \tag{B.24}$$

and

$$v_2(t) = k_2 i|i| + \frac{1}{C}\int i\,dt \tag{B.25}$$

Because of problems similar to those encountered above, approximations must again be made. In this case, the largest portion of the input voltage appears across R_1 except for very large current. Thus, it was assumed that in the steady state,

$$i_{ss} = I \sin \omega t \tag{B.26}$$

TABLE 7.--Describing function of network A

V	ω	0.1	0.2	0.3	0.5	0.7	1.0	2.0	5.0	10.0
2.0	Magnitude	0.267	0.229	0.222	0.218	0.216	0.216	0.215	0.215	0.215
	Angle	-27.66°	-15.93°	-10.96°	- 6.68°	- 4.80°	- 3.37°	- 1.69°	- 0.68°	- 0.34°
2.5	Magnitude	0.242	0.208	0.201	0.197	0.196	0.195	0.195	0.195	0.195
	Angle	-28.51°	-16.37°	-11.25°	- 6.85°	- 4.92°	- 3.45°	- 1.73°	- 0.69°	- 0.35°
3.0	Magnitude	0.223	0.192	0.185	0.182	0.181	0.181	0.180	0.180	0.180
	Angle	-29.16°	-16.70°	-11.47°	- 6.99°	- 5.02°	- 3.52°	- 1.76°	- 0.71°	- 0.35°
4.0	Magnitude	0.196	0.168	0.162	0.159	0.159	0.158	0.158	0.158	0.158
	Angle	-30.10°	-17.16°	-11.78°	- 7.18°	- 5.15°	- 3.61°	- 1.80°	- 0.72°	- 0.36°
5.0	Magnitude	0.177	0.152	0.146	0.144	0.143	0.142	0.142	0.142	0.142
	Angle	-30.77°	-17.49°	-12.01°	- 7.31°	- 5.25°	- 3.68°	- 1.84°	- 0.74°	- 0.37°
10.0	Magnitude	0.128	0.110	0.106	0.104	0.103	0.103	0.103	0.103	0.103
	Angle	-32.45°	-18.34°	-12.57°	- 7.65°	- 5.49°	- 3.85°	- 1.93°	- 0.77°	- 0.39°
20.0	Magnitude	0.092	0.079	0.076	0.075	0.075	0.074	0.074	0.074	0.074
	Angle	-33.69°	-18.96°	-12.98°	- 7.89°	- 5.67°	- 3.97°	- 1.99°	- 0.80°	- 0.40°
40.0	Magnitude	0.066	0.056	0.054	0.053	0.053	0.053	0.053	0.053	0.053
	Angle	-34.60°	-19.41°	-13.28°	- 8.08°	- 5.80°	- 4.06°	- 2.04°	- 0.81°	- 0.41°
80.0	Magnitude	0.047	0.040	0.039	0.038	0.038	0.038	0.038	0.038	0.038
	Angle	-35.25°	-19.74°	-13.50°	- 8.21°	- 5.89°	- 4.13°	- 2.07°	- 0.83°	- 0.41°

The Fourier series for $i_{ss}|i_{ss}|$ is then

$$i_{ss}|i_{ss}| = I^2(b_1 \sin \omega t + b_3 \sin 3\omega t + b_5 \sin 5\omega t + \cdots) \qquad (B.27)$$

where

$$b_n = \frac{4}{\pi}\int_0^{\pi/2} \sin^2 \omega t (\sin n\omega t)\, d(\omega t)$$

$$= \frac{2}{\pi}\int_0^{\pi/2} (\sin nx - \sin nx \cos 2x)\, dx$$

$$= -\frac{8}{\pi}\left[\frac{1}{n(n^2-4)}\right] . \qquad (B.28)$$

$$b_1 = \frac{8}{3\pi} \quad , \quad b_3 = \frac{-8}{15\pi} \quad , \quad b_5 = \frac{-8}{105\pi} \qquad (B.29)$$

Thus,

$$i_{ss}|i_{ss}| = \frac{8I^2}{3\pi}\left(\sin \omega t - \frac{1}{5}\sin 3\omega t - \frac{1}{35}\sin 5\omega t - \cdots\right) \qquad (B.30)$$

Neglecting all but the fundamental term,

$$V \sin(\omega t - \theta) = R_1 I \sin \omega t + \frac{8k_2}{3\pi} I^2 \sin \omega t - \frac{I}{\omega C} \cos \omega t \qquad (B.31)$$

This leads to the equations:

$$V = \sqrt{\left(\frac{8k_2}{3\pi} I^2 + R_1 I\right)^2 + \left(\frac{I}{\omega C}\right)^2} \qquad (B.32)$$

and $$\Theta = \cot^{-1}\left[\omega C\left(\frac{8k_2 I}{3\pi} + R_1\right)\right] \qquad (B.33)$$

Equation (B.32) may be rewritten:

$$I^4 + \frac{3\pi R_1}{4k_2} I^3 + \frac{9\pi^2}{64k_2^2}\left[R_1^2 + \left(\frac{1}{\omega C}\right)^2\right] I^2 - \frac{9\pi^2}{64k_2^2} V^2 = 0 \qquad (B.34)$$

Values for R_1, k_2, and C are inserted and the equation is solved for various combinations of V and ω .

Then,

$$v_{2ss} = \frac{8k_2 I^2}{3\pi} \sin \omega t - \frac{I}{\omega C} \cos \omega t \qquad (B.35)$$

$$= V_2 \sin(\omega t - \phi) \qquad (B.36)$$

where

$$V_2 = I\sqrt{\left(\frac{8k_2 I}{3\pi}\right)^2 + \left(\frac{1}{\omega C}\right)^2} \qquad (B.37)$$

and $$\phi = \cot^{-1}\left(\frac{8k_2 \omega C I}{3\pi}\right) \qquad (B.38)$$

As before, the describing function is then found from equation (B.8).

Table 8 gives the describing function for network B.

TABLE 8.--Describing function of network B

V	ω	0.1	0.2	0.3	0.5	0.7	1.0	2.0	5.0	10.0
1	Magnitude	0.053	0.027	0.018	0.011	0.008	0.006	0.004	0.003	0.003
	Angle	-83.49°	-81.58°	-78.70°	-72.57°	-66.63°	-58.54°	-39.45°	-18.25°	- 9.37°
3	Magnitude	0.054	0.028	0.020	0.014	0.012	0.011	0.010	0.010	0.010
	Angle	-76.76°	-68.69°	-60.63°	-47.41°	-38.01°	-28.76°	-15.38°	- 6.28°	- 3.15°
5	Magnitude	0.055	0.031	0.024	0.019	0.017	0.017	0.016	0.016	0.016
	Angle	-70.40°	-57.63°	-47.12°	-33.20°	-25.12°	-18.20°	- 9.35°	- 3.77°	- 1.89°
10	Magnitude	0.060	0.040	0.035	0.032	0.031	0.031	0.031	0.031	0.030
	Angle	-56.60°	-38.92°	-28.58°	-18.20°	-13.24°	- 9.36°	- 4.72°	- 1.89°	- 0.95°
20	Magnitude	0.076	0.063	0.060	0.059	0.058	0.058	0.058	0.058	0.058
	Angle	-38.34°	-22.20°	-15.31°	- 9.34°	- 6.71°	- 4.71°	- 2.36°	- 0.94°	- 0.47°
40	Magnitude	0.114	0.107	0.105	0.105	0.104	0.104	0.104	0.104	0.104
	Angle	-22.00°	-11.58°	- 7.81°	- 4.71°	- 3.37°	- 2.36°	- 1.18°	- 0.47°	- 0.23°
60	Magnitude	0.150	0.145	0.144	0.143	0.143	0.143	0.143	0.143	0.143
	Angle	-15.17°	- 7.80°	- 5.22°	- 3.14°	- 2.24°	- 1.58°	- 0.79°	- 0.32°	- 0.15°
80	Magnitude	0.181	0.178	0.177	0.177	0.176	0.176	0.176	0.176	0.176
	Angle	-11.53°	- 5.88°	- 3.93°	- 2.36°	- 1.69°	- 1.18°	- 0.59°	- 0.24°	- 0.11°
100	Magnitude	0.212	0.206	0.206	0.205	0.205	0.205	0.205	0.205	0.205
	Angle	- 9.29°	- 4.70°	- 3.15°	- 1.89°	- 1.34°	- 0.94°	- 0.47°	- 0.19°	- 0.10°

TABLE 7.--Describing function of network A

V	ω	0.1	0.2	0.3	0.5	0.7	1.0	2.0	5.0	10.0
2.0	Magnitude	0.267	0.229	0.222	0.218	0.216	0.216	0.215	0.215	0.215
	Angle	-27.66°	-15.93°	-10.96°	- 6.68°	- 4.80°	- 3.37°	- 1.69°	- 0.68°	- 0.34°
2.5	Magnitude	0.242	0.208	0.201	0.197	0.196	0.195	0.195	0.195	0.195
	Angle	-28.51°	-16.37°	-11.25°	- 6.85°	- 4.92°	- 3.45°	- 1.73°	- 0.69°	- 0.35°
3.0	Magnitude	0.223	0.192	0.185	0.182	0.181	0.181	0.180	0.180	0.180
	Angle	-29.16°	-16.70°	-11.47°	- 6.99°	- 5.02°	- 3.52°	- 1.76°	- 0.71°	- 0.35°
4.0	Magnitude	0.196	0.168	0.162	0.159	0.159	0.158	0.158	0.158	0.158
	Angle	-30.10°	-17.16°	-11.78°	- 7.18°	- 5.15°	- 3.61°	- 1.80°	- 0.72°	- 0.36°
5.0	Magnitude	0.177	0.152	0.146	0.144	0.143	0.142	0.142	0.142	0.142
	Angle	-30.77°	-17.49°	-12.01°	- 7.31°	- 5.25°	- 3.68°	- 1.84°	- 0.74°	- 0.37°
10.0	Magnitude	0.128	0.110	0.106	0.104	0.103	0.103	0.103	0.103	0.103
	Angle	-32.45°	-18.34°	-12.57°	- 7.65°	- 5.49°	- 3.85°	- 1.93°	- 0.77°	- 0.39°
20.0	Magnitude	0.092	0.079	0.076	0.075	0.075	0.074	0.074	0.074	0.074
	Angle	-33.69°	-18.96°	-12.98°	- 7.89°	- 5.67°	- 3.97°	- 1.99°	- 0.80°	- 0.40°
40.0	Magnitude	0.066	0.056	0.054	0.053	0.053	0.053	0.053	0.053	0.053
	Angle	-34.60°	-19.41°	-13.28°	- 8.08°	- 5.80°	- 4.06°	- 2.04°	- 0.81°	- 0.41°
80.0	Magnitude	0.047	0.040	0.039	0.038	0.038	0.038	0.038	0.038	0.038
	Angle	-35.25°	-19.74°	-13.50°	- 8.21°	- 5.89°	- 4.13°	- 2.07°	- 0.83°	- 0.41°

The Fourier series for $i_{ss}|i_{ss}|$ is then

$$i_{ss}|i_{ss}| = I^2(b_1 \sin \omega t + b_3 \sin 3\omega t + b_5 \sin 5\omega t + \cdots) \qquad (B.27)$$

where

$$b_n = \frac{4}{\pi}\int_0^{\pi/2} \sin^2 \omega t (\sin n\omega t)\, d(\omega t)$$

$$= \frac{2}{\pi}\int_0^{\pi/2} (\sin nx - \sin nx \cos 2x)\, dx$$

$$= -\frac{8}{\pi}\left[\frac{1}{n(n^2-4)}\right] . \qquad (B.28)$$

$$b_1 = \frac{8}{3\pi} \quad , \quad b_3 = \frac{-8}{15\pi} \quad , \quad b_5 = \frac{-8}{105\pi} \qquad (B.29)$$

Thus,

$$i_{ss}|i_{ss}| = \frac{8I^2}{3\pi}\left(\sin \omega t - \frac{1}{5}\sin 3\omega t - \frac{1}{35}\sin 5\omega t - \cdots\right) \qquad (B.30)$$

Neglecting all but the fundamental term,

$$V \sin(\omega t - \theta) = R_1 I \sin \omega t + \frac{8k_2}{3\pi} I^2 \sin \omega t - \frac{I}{\omega C}\cos \omega t \qquad (B.31)$$

This leads to the equations:

$$V = \sqrt{\left(\frac{8k_2}{3\pi} I^2 + R_1 I\right)^2 + \left(\frac{I}{\omega C}\right)^2} \qquad (B.32)$$

and $$\Theta = \cot^{-1}\left[\omega C\left(\frac{8k_2 I}{3\pi} + R_1\right)\right] \qquad (B.33)$$

Equation (B.32) may be rewritten:

$$I^4 + \frac{3\pi R_1}{4k_2} I^3 + \frac{9\pi^2}{64k_2^2}\left[R_1^2 + \left(\frac{1}{\omega C}\right)^2\right] I^2 - \frac{9\pi^2}{64k_2^2} V^2 = 0 \qquad (B.34)$$

Values for R_1, k_2, and C are inserted and the equation is solved for various combinations of V and ω.

Then,

$$v_{2ss} = \frac{8k_2 I^2}{3\pi} \sin \omega t - \frac{I}{\omega C} \cos \omega t \qquad (B.35)$$

$$= V_2 \sin(\omega t - \phi) \qquad (B.36)$$

where

$$V_2 = I\sqrt{\left(\frac{8k_2 I}{3\pi}\right)^2 + \left(\frac{1}{\omega C}\right)^2} \qquad (B.37)$$

and $$\phi = \cot^{-1}\left(\frac{8k_2 \omega C I}{3\pi}\right) \qquad (B.38)$$

As before, the describing function is then found from equation (B.8).

Table 8 gives the describing function for network B.

TABLE 8.--Describing function of network B

V	ω	0.1	0.2	0.3	0.5	0.7	1.0	2.0	5.0	10.0
1	Magnitude	0.053	0.027	0.018	0.011	0.008	0.006	0.004	0.003	0.003
	Angle	-83.49°	-81.58°	-78.70°	-72.57°	-66.63°	-58.54°	-39.45°	-18.25°	- 9.37°
3	Magnitude	0.054	0.028	0.020	0.014	0.012	0.011	0.010	0.010	0.010
	Angle	-76.76°	-68.69°	-60.63°	-47.41°	-38.01°	-28.76°	-15.38°	- 6.28°	- 3.15°
5	Magnitude	0.055	0.031	0.024	0.019	0.017	0.017	0.016	0.016	0.016
	Angle	-70.40°	-57.63°	-47.12°	-33.20°	-25.12°	-18.20°	- 9.35°	- 3.77°	- 1.89°
10	Magnitude	0.060	0.040	0.035	0.032	0.031	0.031	0.031	0.031	0.030
	Angle	-56.60°	-38.92°	-28.58°	-18.20°	-13.24°	- 9.36°	- 4.72°	- 1.89°	- 0.95°
20	Magnitude	0.076	0.063	0.060	0.059	0.058	0.058	0.058	0.058	0.058
	Angle	-38.34°	-22.20°	-15.31°	- 9.34°	- 6.71°	- 4.71°	- 2.36°	- 0.94°	- 0.47°
40	Magnitude	0.114	0.107	0.105	0.105	0.104	0.104	0.104	0.104	0.104
	Angle	-22.00°	-11.58°	- 7.81°	- 4.71°	- 3.37°	- 2.36°	- 1.18°	- 0.47°	- 0.23°
60	Magnitude	0.150	0.145	0.144	0.143	0.143	0.143	0.143	0.143	0.143
	Angle	-15.17°	- 7.80°	- 5.22°	- 3.14°	- 2.24°	- 1.58°	- 0.79°	- 0.32°	- 0.15°
80	Magnitude	0.181	0.178	0.177	0.177	0.176	0.176	0.176	0.176	0.176
	Angle	-11.53°	- 5.88°	- 3.93°	- 2.36°	- 1.69°	- 1.18°	- 0.59°	- 0.24°	- 0.11°
100	Magnitude	0.212	0.206	0.206	0.205	0.205	0.205	0.205	0.205	0.205
	Angle	- 9.29°	- 4.70°	- 3.15°	- 1.89°	- 1.34°	- 0.94°	- 0.47°	- 0.19°	- 0.10°

Network C

Refer to Figure 4, page 5, for a schematic of network C. Assuming an input voltage of the form

$$v_1(t) = V \sin(\omega t - \theta) \tag{B.39}$$

the equations for the circuit are

$$V \sin(\omega t - \theta) = (k_1 + k_2) i|i| + \frac{1}{C}\int i\,dt \tag{B.40}$$

and

$$v_2(t) = k_2 i|i| + \frac{1}{C}\int i\,dt \tag{B.41}$$

In this case, the largest portion of the input voltage appears across the nonlinear elements and the same approximation is made as for network A,

$$i_{ss}|i_{ss}| = I^2 \sin \omega t \tag{B.42}$$

Then,

$$i_{ss} = \frac{2}{\sqrt{\pi}} \frac{\Gamma(1.25)}{\Gamma(1.75)} \left(\sin \omega t + \frac{1}{7} \sin 3\omega t + \frac{5}{77} \sin 5\omega t + \cdots\right) I \tag{B.43}$$

Neglecting the harmonics,

$$V \sin(\omega t - \theta) = (k_1 + k_2) I^2 \sin \omega t - \frac{2}{\sqrt{\pi}} \frac{\Gamma(1.25)}{\Gamma(1.75)} \frac{I}{\omega C} \cos \omega t \tag{B.44}$$

This leads to two other equations:

$$V = \sqrt{(k_1 + k_2)^2 I^4 + \left[\frac{2}{\sqrt{\pi}} \frac{\Gamma(1.25)}{\Gamma(1.75)} \frac{I}{\omega C}\right]^2} \qquad (B.45)$$

and $$\theta = \cot^{-1}\left[\frac{\sqrt{\pi}}{2} \frac{\Gamma(1.75)}{\Gamma(1.25)} (k_1 + k_2) \omega C I\right] \qquad (B.46)$$

Rewriting equation (B.45),

$$I^4 + \frac{1.2384033473}{(k_1 + k_2)^2 (\omega C)^2} I^2 - \frac{V^2}{(k_1 + k_2)^2} = 0 \qquad (B.47)$$

Numerical values are inserted for k_1, k_2, and C; and solutions of the equation are found for various combinations of V and ω.

Then,

$$v_{2ss} = k_2 I^2 \sin \omega t - \frac{2}{\sqrt{\pi}} \frac{\Gamma(1.25)}{\Gamma(1.75)} \frac{I}{\omega C} \cos \omega t \qquad (B.48)$$

$$= V_2 \sin(\omega t - \phi) \qquad (B.49)$$

where

$$V_2 = I\sqrt{(k_2 I)^2 + \left[\frac{2}{\sqrt{\pi}} \frac{\Gamma(1.25)}{\Gamma(1.75)} \frac{1}{\omega C}\right]^2} \qquad (B.50)$$

$$\phi = \cot^{-1}\left[\frac{\sqrt{\pi}}{2} \frac{\Gamma(1.75)}{\Gamma(1.25)} k_2 I \omega C\right] \qquad (B.51)$$

The describing function is then found from equation (B.8).

Table 9 gives the describing function for network C.

TABLE 9.--Describing function of network G

V	ω	0.1	0.2	0.3	0.5	0.7	1.0	2.0	5.0	10.0
1	Magnitude	0.253	0.141	0.106	0.083	0.076	0.071	0.068	0.067	0.067
	Angle	-61.13°	-54.93°	-46.72°	-34.14°	-26.15°	-19.14°	- 9.91°	- 4.01°	- 2.01°
3	Magnitude	0.157	0.098	0.082	0.073	0.070	0.068	0.067	0.067	0.067
	Angle	-57.01°	-43.05°	-32.97°	-21.68°	-15.94°	-11.35°	- 5.74°	- 2.30°	- 1.16°
5	Magnitude	0.129	0.087	0.076	0.070	0.068	0.068	0.067	0.067	0.067
	Angle	-52.80°	-36.67°	-26.97°	-17.19°	-12.50°	- 8.84°	- 4.45°	- 1.78°	- 0.90°
10	Magnitude	0.103	0.077	0.072	0.068	0.068	0.067	0.067	0.067	0.067
	Angle	-45.26°	-28.30°	-19.98°	-12.38°	- 8.93°	- 6.28°	- 3.15°	- 1.26°	- 0.63°
20	Magnitude	0.087	0.072	0.069	0.068	0.067	0.067	0.067	0.067	0.067
	Angle	-36.69°	-21.10°	-14.49°	- 8.84°	- 6.34°	- 4.45°	- 2.23°	- 0.90°	- 0.45°
40	Magnitude	0.077	0.070	0.068	0.067	0.067	0.067	0.067	0.067	0.067
	Angle	-28.30°	-15.31°	-10.38°	- 6.28°	- 4.50°	- 3.15°	- 1.58°	- 0.63°	- 0.32°
80	Magnitude	0.072	0.068	0.067	0.067	0.067	0.067	0.067	0.067	0.067
	Angle	-21.10°	-10.99°	- 7.39°	- 4.45°	- 3.18°	- 2.23°	- 1.12°	- 0.45°	- 0.23°

APPENDIX C

ANALOG COMPUTER SIMULATION

The analog computer setups used in simulating the various closed-loop system are discussed in this appendix.

The computer used in the simulation was the Donner Scientific Company Model 3400 Analog Computer. The Donner Model 3750 Variable Base Function Generator was used to simulate the necessary non-linear characteristics. The recording was done by means of a two channel Brush Recorder, Model BL-222. The pen motors of the recorder were driven directly by the computer amplifiers, eliminating the need for an additional amplifier.

I. LINEAR SYSTEM

The transfer function of equation (C.1) was simulated by the computer setup shown in Figure 31, page 70.

$$\frac{E_o(s)}{E_i(s)} = \frac{A}{S^2 + 2S + 2} \qquad (C.1)$$

This may be verified as follows:

$$e_o = -\frac{1}{.5}\int e_2\,dt - \frac{1}{.5}\int e_o\,dt$$

$$e_o = -2\int\left[-\frac{1}{R}\int e_i\,dt - \int(-e_o)\,dt\right]dt - 2\int e_o\,dt$$

$$e_o = \frac{2}{R}\iint e_i\,dt - 2\iint e_o\,dt - 2\int e_o\,dt \qquad (C.2)$$

Assuming all initial conditions are zero and writing the Laplace transform,

$$E_o(s) = \frac{2}{R}\frac{E_i(s)}{s^2} - \frac{2E_o(s)}{s^2} - \frac{2E_o(s)}{s}$$

$$s^2 E_o(s) = \frac{2}{R}E_i(s) - 2E_o(s) - 2sE_o(s)$$

$$\frac{E_o(s)}{E_i(s)} = \frac{2/R}{s^2+2s+2} = \frac{A}{s^2+2s+2} \qquad (C.3)$$

The computer setup for the simulation of

$$\frac{E_o(s)}{E_i(s)} = -\frac{1}{15}\frac{s+.075}{s+.005} \qquad (C.4)$$

is shown in Figure 32. This is verified thus:

$$e_o = -\frac{1}{20}e_3 - \frac{1}{15}e_i = \frac{1}{20}e_2 - \frac{1}{15}e_i$$

$$e_o = \frac{1}{20}\left[-\frac{1}{10}\int e_o\,dt - \frac{1}{10}\int e_i\,dt\right] - \frac{1}{15}e_i$$

$$e_o = -\frac{1}{200}\int e_o\,dt - \frac{1}{200}\int e_i\,dt - \frac{1}{15}e_i \qquad (C.5)$$

The Laplace transform is taken, assuming zero initial conditions.

$$E_o(s) = \frac{-E_o(s)}{200s} - \frac{E_i(s)}{200s} - \frac{E_i(s)}{15}$$

$$sE_o(s) = \frac{-E_o(s)}{200} - \frac{E_i(s)}{15}\left[s + \frac{15}{200}\right]$$

$$\frac{E_o(s)}{E_i(s)} = -\frac{1}{15}\frac{s+.075}{s+.005} \qquad (C.6)$$

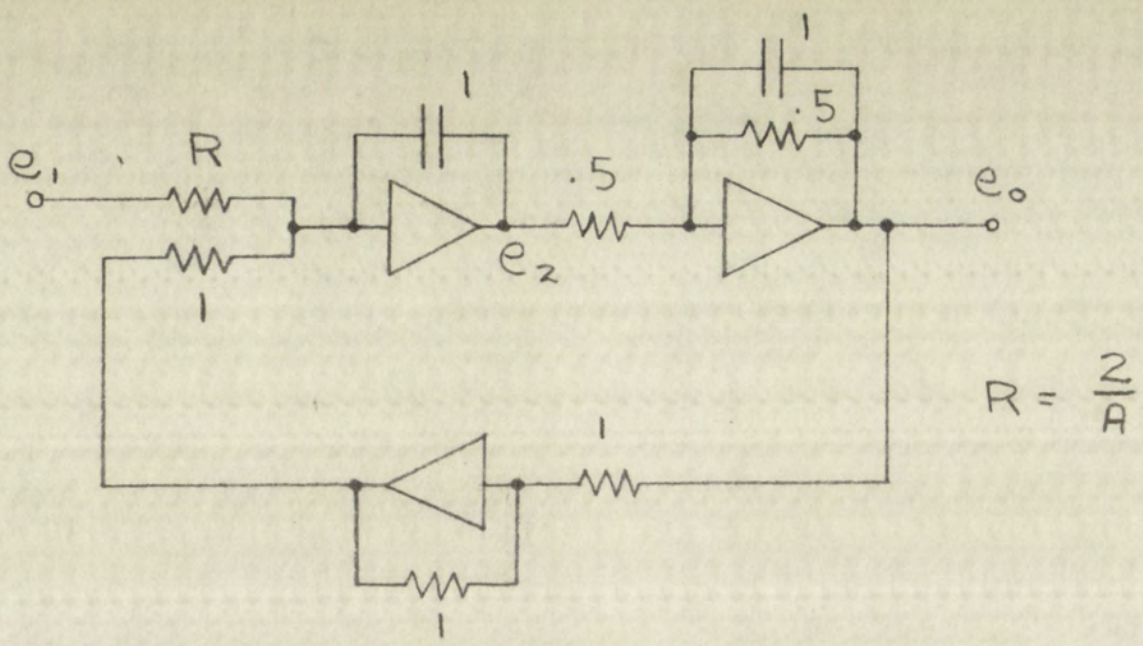

Figure 31.--Computer simulation of $\frac{E_o(s)}{E_1(s)} = \frac{A}{s^2+2s+2}$

Note to Figures 31 and 32:

Resistances in megohms

Capacitances in microfarads

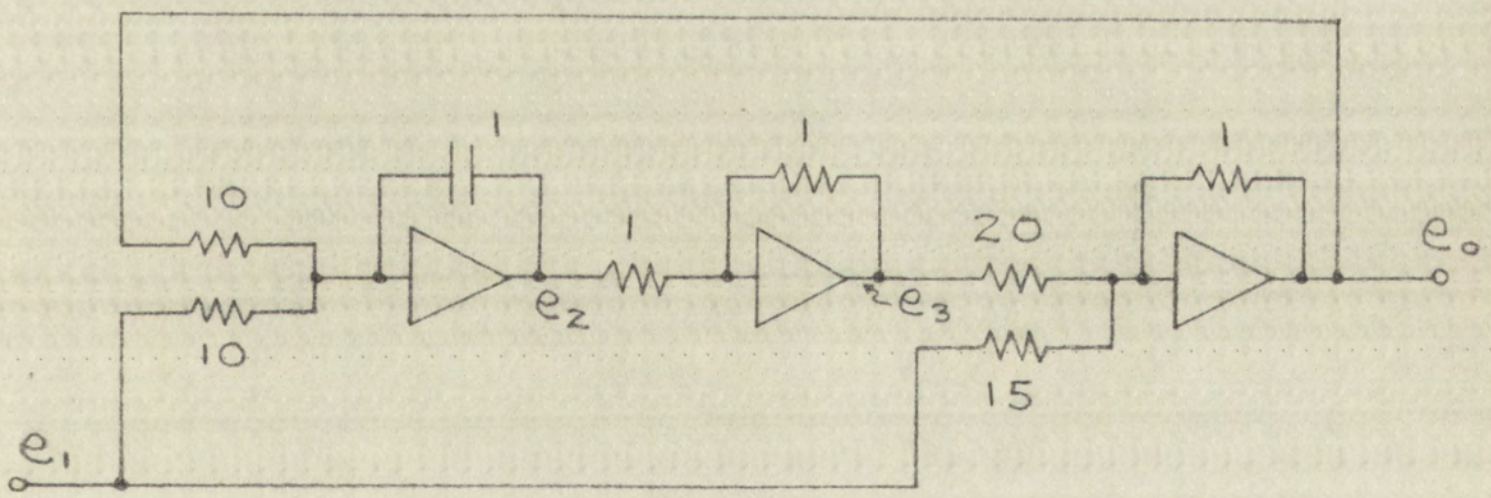

Figure 32.--Computer simulation of $\frac{E_o(s)}{E_1(s)} = -\frac{1}{15}\frac{s+.075}{s+.005}$

The computer setup for simulating the closed-loop system resulting from the use of the network in Figure 3, page 3, as compensation for the system in Figure 2, page 3, is shown in Figure 33.

II. NONLINEAR SYSTEMS

In simulating the different nonlinear systems it was necessary to obtain two nonlinear input-output characteristics. The first required that for an input of $x|x|$, the output be directly proportional to x. The second required that for an input of x, the output be directly proportional to $x|x|$. Mathematical expressions of these two characteristics, including constants of proportionality, are given in equations (C.7) and (C.8).

$$y = 8.944 \sqrt{|x|}\ \frac{x}{|x|} \qquad (C.7)$$

$$y = .0125\, x|x| \qquad (C.8)$$

Straight line approximations to both of these curves were obtained by using the variable base function generator. Table 10, page 73, gives the values of input and output voltage at the break points of the approximation to equation (C.7). Table 11, page 73, gives the same information for the approximation to equation (C.8). In both cases, only the positive half of the curve is considered, since both are symmetrical about the origin.

By using these straight line approximations it was possible

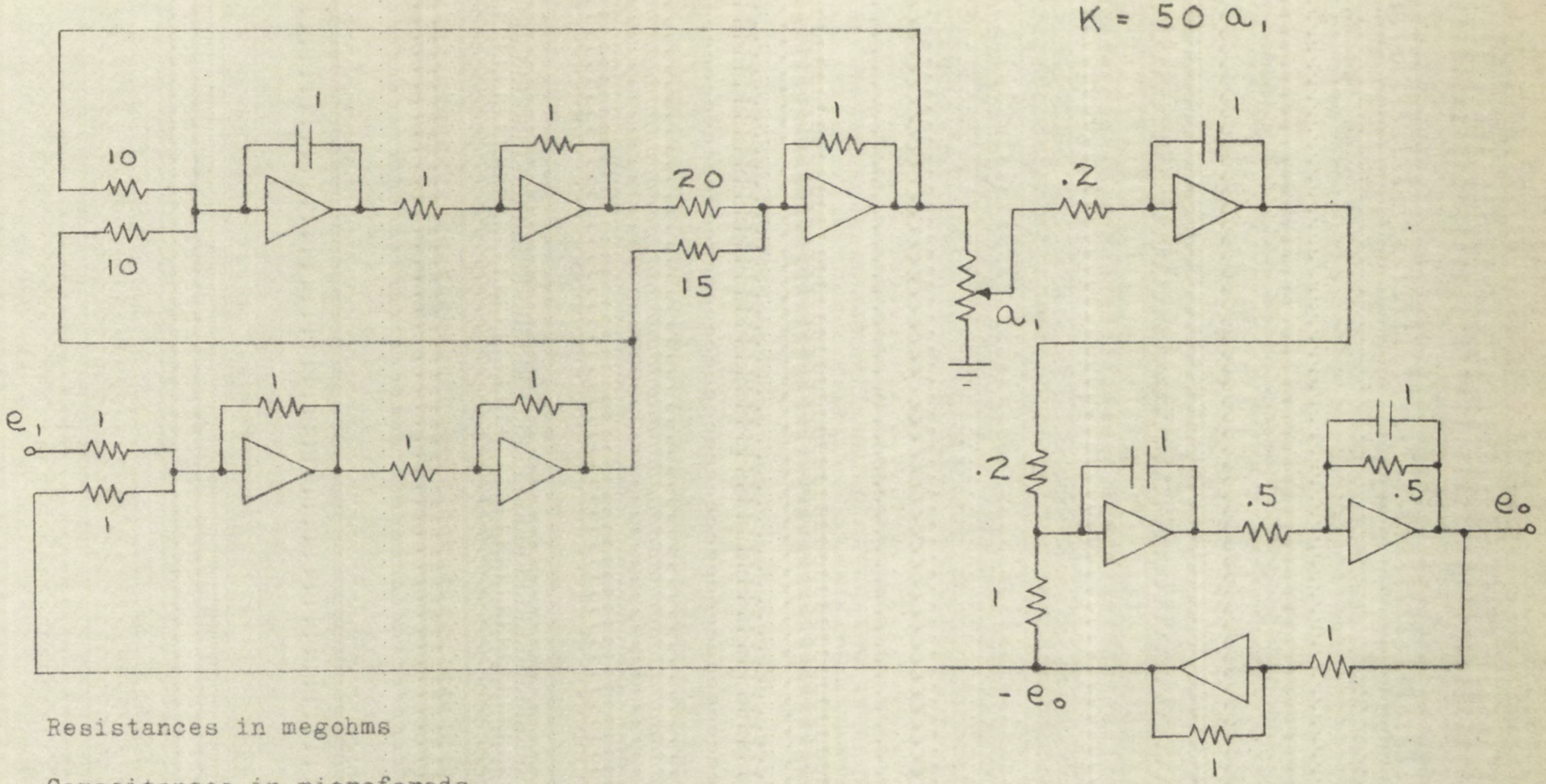

Resistances in megohms

Capacitances in microfarads

Figure 33.--Computer simulation of closed-loop system with linear compensation network

TABLE 10.--Break point voltages of straight line approximation to

$$y = 8.944 \sqrt{|x|}\ \frac{x}{|x|}$$

Input voltage	Output voltage
0	0
+ 1.5	+10.0
+ 6.0	+22.1
+10.0	+28.4
+15.0	+34.8
+25.0	+45.0
+40.0	+56.8
+60.0	+69.4
+80.0	+80.2

TABLE 11.--Break point voltages of straight line approximation to

$$y = .0125\ x\ |x|$$

Input voltage	Output voltage
0	0
+ 5.0	+ 0.3
+10.0	+ 1.2
+15.0	+ 2.8
+20.0	+ 5.0
+25.0	+ 7.8
+30.0	+11.2
+35.0	+15.3
+40.0	+20.0
+50.0	+31.0
+60.0	+45.0
+70.0	+61.4
+80.0	+80.0

to simulate the three nonlinear networks of Figure 4, page 5.

Network A

The equations for this network, shown in Figure 4, page 5, are:

$$v_1 = k_1 i|i| + R_2 i + \frac{1}{C}\int i\,dt \qquad (C.9)$$

and

$$v_2 = R_2 i + \frac{1}{C}\int i\,dt \qquad (C.10)$$

In order to set up these equations on the computer, it was necessary to do some amplitude scaling. This was done by letting $i = \alpha I$ or $I = i/\alpha$. Equation (C.9) becomes

$$v_1 = \alpha^2 k_1 I|I| + R_2 \alpha I + \frac{\alpha}{C}\int I\,dt \qquad (C.11)$$

or

$$I|I| = \frac{v_1}{\alpha^2 k_1} - \frac{R_2 I}{\alpha k_1} - \frac{1}{\alpha k_1 C}\int I\,dt \qquad (C.12)$$

This equation was then set up on the computer. The output voltage was then

$$v_2 = \alpha R_2 I + \frac{\alpha}{C}\int I\,dt \qquad (C.13)$$

The computer wiring diagram for simulating the closed-loop system of Figure 2, page 3, with network A as compensation is shown in Figure 34.

Since the function generator was set up for an input between -80 volts and +80 volts, it was necessary to choose α so that

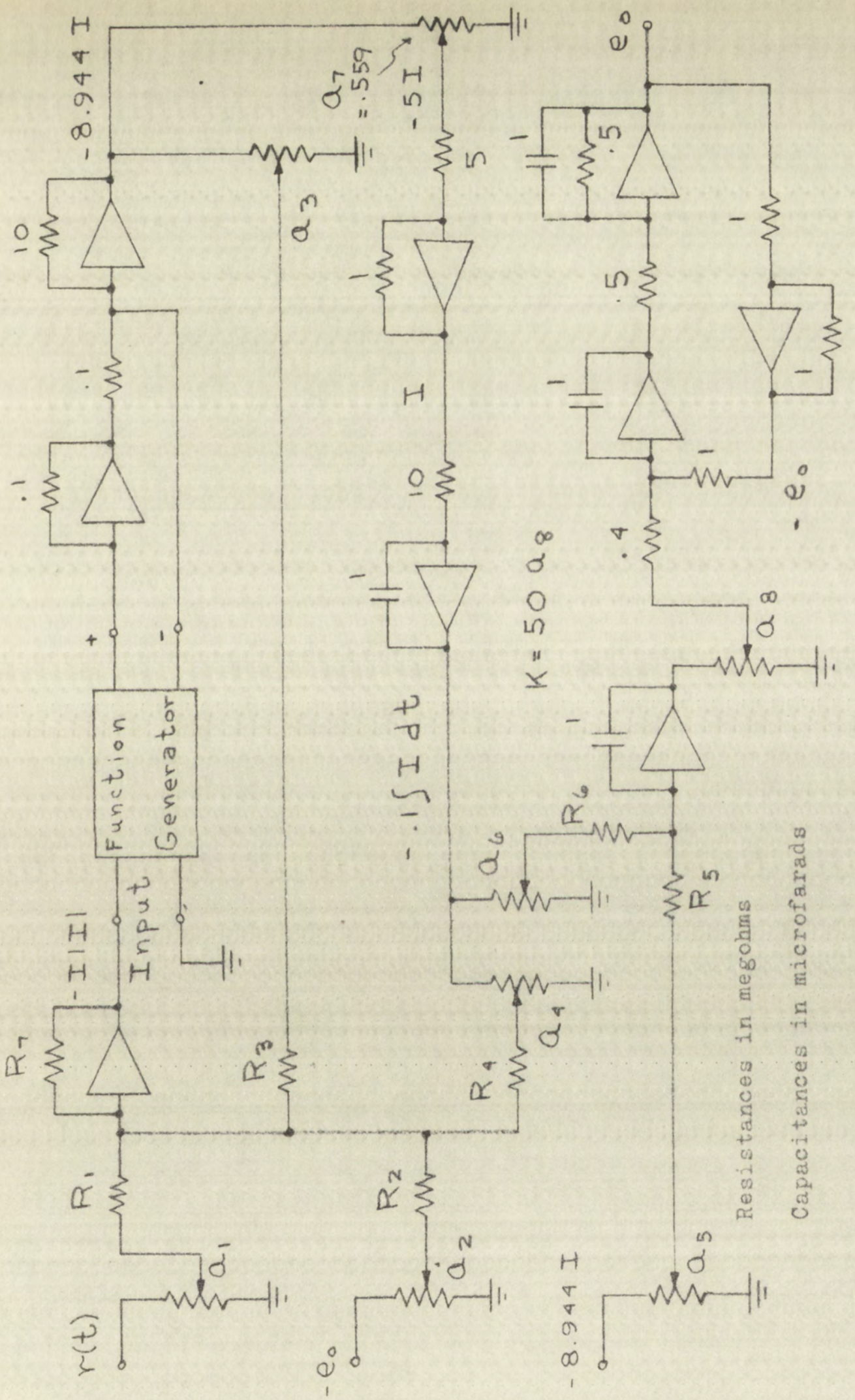

Resistances in megohms

Capacitances in microfarads

Figure 34.--Computer simulation of system A

$-80 \leq I|I| \leq +80$. Thus, the value of α which was chosen depended on the range of values for v_1.

The calculation of the values of R_1 through R_7 and a_1 through a_8 necessary to simulate equation (C.12) completed the problem.

Network B

The equations for network B, shown in Figure 4, page 5, are:

$$v_1 = R_1 i + k_2 i|i| + \frac{1}{C}\int i\,dt \qquad (C.14)$$

and

$$v_2 = k_2 i|i| + \frac{1}{C}\int i\,dt \qquad (C.15)$$

As above, if $i = \alpha I$, equation (C.14) becomes

$$v_1 = \alpha R_1 I + \alpha^2 k_2 I|I| + \frac{\alpha}{C}\int I\,dt \qquad (C.16)$$

or

$$I = \frac{v_1}{\alpha R_1} - \frac{\alpha k_2}{R_1} I|I| - \frac{1}{R_1 C}\int I\,dt \qquad (C.17)$$

This equation was programmed on the computer. Then,

$$v_2 = \alpha^2 k_2 I|I| + \frac{\alpha}{C}\int I\,dt \qquad (C.18)$$

The wiring diagram for the closed-loop system with network B as compensation is shown in Figure 35.

In this case it was necessary to choose α such that $-80 \leq I \leq +80$ for the desired range of v_1. Using the chosen value of α, the values of R_1 through R_7 and a_1 through a_7 necessary to simulate equation (C.17) were calculated.

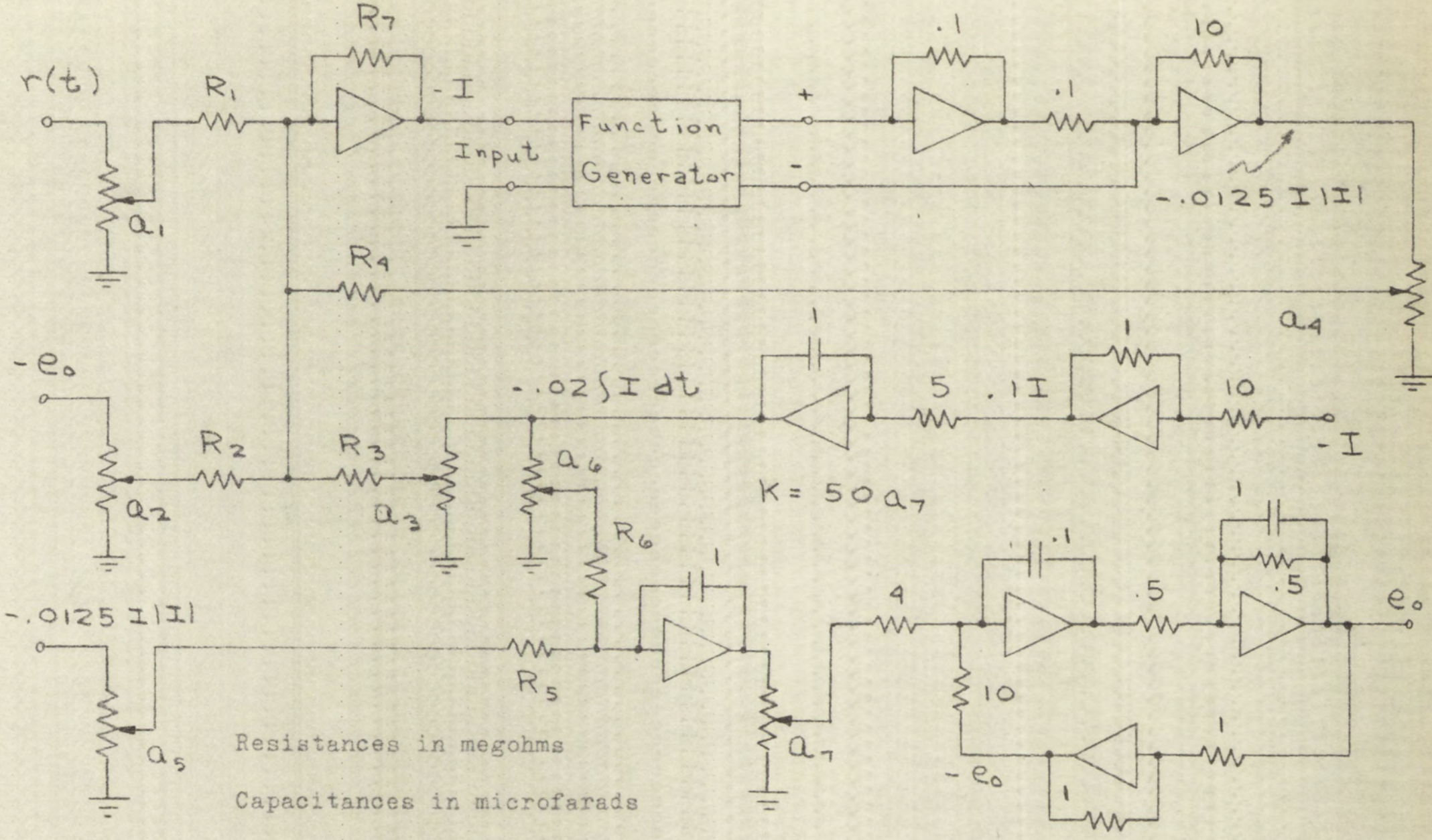

Figure 35.--Computer simulation of system B

The step responses for this system are such that it was advantageous to speed up the solution by a factor of five. This was done by increasing the gain of each integrating unit in Figure 35 by five times.

Network C

The equations for network C, shown in Figure 4, page 5, are:

$$v_1 = (k_1 + k_2)\, i|i| + \frac{1}{C}\int i\, dt \qquad (C.19)$$

and

$$v_2 = k_2\, i|i| + \frac{1}{C}\int i\, dt \qquad (C.20)$$

If $i = \alpha I$, equation (C.19) becomes

$$v_1 = \alpha^2(k_1 + k_2)\, I|I| + \frac{\alpha}{C}\int I\, dt \qquad (C.21)$$

or

$$I|I| = \frac{v_1}{\alpha^2(k_1+k_2)} - \frac{1}{\alpha(k_1+k_2)C}\int I\, dt \qquad (C.22)$$

This equation was set up on the computer. Then,

$$v_2 = \alpha^2 k_2\, I|I| + \frac{\alpha}{C}\int I\, dt \qquad (C.23)$$

The wiring diagram for the closed-loop system with network B is shown in Figure 36.

As with network A, α was chosen so that $-80 \leq I|I| \leq +80$. The proper values of R_1 through R_6 and a_1 through a_7 were then calculated.

In view of the preceding discussion, it is now possible to

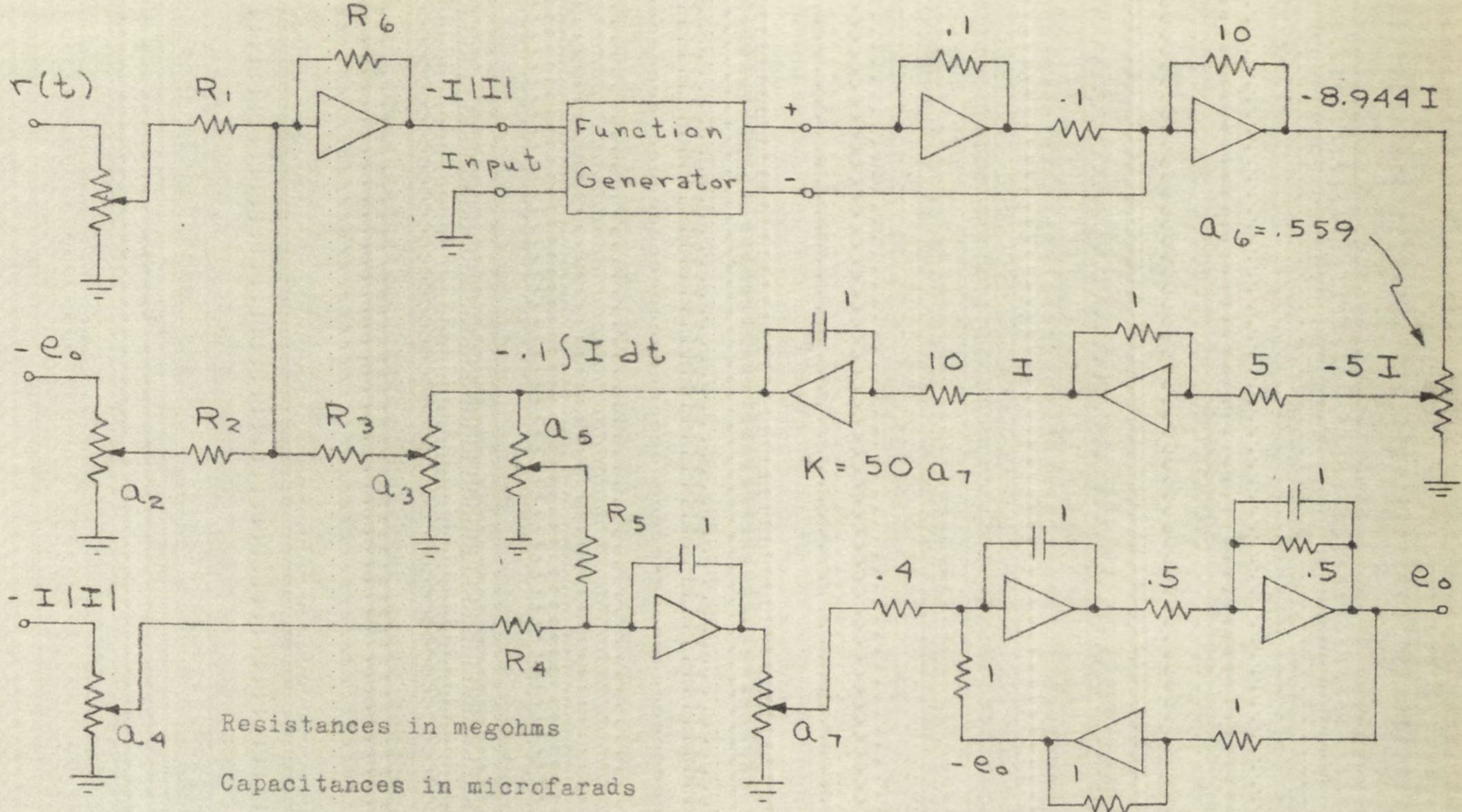

Figure 36.--Computer simulation of system C

elucidate further concerning a point which was mentioned briefly in Chapter III. From the nature of the straight line approximations given in Tables 10 and 11, page 73, it is obvious that the entire eighty volt range should be utilized to obtain the best approximations to equation (C.7) and (C.8). For this reason, the determination of the limit cycle frequencies and amplitudes was most accurate when the computer setup was scaled specifically for the expected amplitude range of the limit cycle.

The limit cycles observed in the larger step-function responses were somewhat inaccurate due to the fact that when the system had settled into the limit cycle, the range of voltages at the function generator input was very small compared to the eighty volt maximum. Thus, the straight line approximations to equations (C.7) and (C.8) were very poor.

IMPORTANT!

Special care should be taken to prevent loss or damage of this volume. If lost or damaged, it must be paid for at the current rate of typing.